UNIVERSITY OF THE WITWATERSRAND
JOHANNESBURG
SCHOOL OF GEOSCIENCES
GEOL.4000 HONOURS
2007

ASINNE TSHIBUBUDZE
0206909M

RELATIVE TIMING OF STRUCTURAL EVENTS: THE MARKOYE FAULT AND ITS ASSOCIATION TO GOLD MINERALISATION

Supervisor: Prof. Kim A.A Hein
Chamber of Mines Chair and Professor of Mining Geology School of Geosciences
University of the Witwatersrand
Johannesburg
Private Bag X3
2050
WITS
South Africa

Declaration

I declare that this dissertation/thesis is my own work. I have correctly acknowledged all the sources, to ideas used in this dissertation/thesis. This dissertation/thesis is submitted for a Bachelor of Science degree with Honours in Geology at the University of the Witwatersrand, Johannesburg. It has not been submitted before in any other university for any examination or degree.

Signature: _____ Date: 29 October 2007

Acknowledgements

This project has been well supported by mining companies including AngloGold Ashanti, Goldfields Mining, Orezone Resources Inc, AMIRA P934 sponsors, University of Ouagadougou, and the University of the Witwatersrand.

I would like to thank AngloGold Ashanti for making the field trip possible by providing the Air flight tickets, medical vaccination and the medical kit.

Thanks to the Orezone Resources Inc and all the employers at Ouagadougou and Essakane offices for accommodating me and my supervisor during the course of the field work, your kind hospitality is much appreciated.

Thanks to the following people who have motivated, guided and helped me when I was completing this work: My supervisor, Prof. Kim, A.A. Hein who guided and gave me a chance to do it for Africa, thank you for your patience, thorough and constructive comments.

Prof. M. Lompo, Mr. Y. Traoré (Chauffeur) for their assistance in field work and organising process.

My sincerer gratitude's to the Orpailleur at Essakane for their time and information during the course of their work.

Thanks to the technician at the University of Ouagadougou who helped me cut the samples into small sizes.

Thanks to the geologists at the Ministere Des Mines, Des carriers et de L'energie of Burkina Faso for the discussion we had pre-field work.

To my family, friends, P. Nkadimeng and all members of Tshanduko Research Group: your patience, support and trust throughout the project were more than valuable.

Finally to God be the glory and honour, for His love, mercy, protection, wisdom and knowledge that guides my footsteps.

Table of Contents

Abstract

The regional lithological and structural mapping completed in the north-eastern part of Burkina Faso indicates that the Essakane goldfield of the West African Craton is hosted by meta-volcanoclastic and meta-sedimentary rocks of the Birimian sequences. The sequences are dominated by meta-volcanoclastic greywackes, intercalated meta-conglomerate, meta-sandstone-greywacke, siltstone and shale. The sequences have primary sedimentary structures preserved as compositional layering.

The depositional environment of the sequences is interpreted to have occurred in a shallow marine continental shelf environment at a delta front setting. The sequences where subjected to several phases of deformation and metamorphism. They have been contact metamorphosed to hornblende hornfels facies during emplacement of adamellite, pyroxenite-gabbro, granodiorite-tonalite plutons, and dolerite dykes.

Structural studies indicate that the NE-trending Markoye fault, which is the first-order crustal-scale structure, have undergone at least two phases of deformation, D1 and D2, with reactivation during the late phase of D2. D1 resulted in formation of NW-trending asymmetric folds and thrusts at Essakane, and the displacement along the Markoye fault was dextral reverse. D2 is a period of SE-NW crustal shortening that formed NE-trending folds, and NE-trending regional foliation. The NE-trending mylonite to ultramylonite zone, pseudotachylyte veins, buck quartz-carbonate (± tourmaline) veins and quartz iron-rich catalasite vein, and late quartz-chlorite shears formed during D2.

D1 is interpreted to pre-date the Eburnean Orogeny, and D2 is correlated to the Eburnean Orogeny ~2.1 G.a. The name ‘Markoye Fault’ should be changed to Markoye Shear Zone (MSZ) to reflect the complex nature of the structure and tectonic history.

Chapter 1: Introduction

1.1 Preamble

The NE-trending Markoye fault in Burkina Faso is a first-order crustal scale structure located in the north-eastern part of Burkina Faso, between the towns of Dori and Tambão by the boarder with Mali and Niger (Fig. 1). The structure has been interpreted as a major westerly-dipping thrust (Milési et al., 1992; Hottin and Ouedraogo, 1992). Delfour and Jeabrum (1970) in Rogers and Dong (2000) defined the structure as an east-verging thrust and BHP geologists interpreted the structure as part of a regional dextral strike-slip system. Castaing et al. (2003) interpreted the same structure as a sinistral fault system, and Milési et al. (1991, 1992), Hirdes and Davis (1998), and Hirdes et al. (1996) interpreted that the Markoye fault formed during the Eburnean Orogeny at 2150 to 2095 Ma. However little field data has been presented to quantify the tectonic history of the structure and thus tectonic interpretation are contradictory.

The focus of this research is the Markoye fault and its tectonic history. Added to this, field studies test the possibility that the Markoye fault is a Pan African structure and that gold metallogenesis is associated with late Neo-Proterozoic Pan African tectonics (c.f. Liégeois et al., 2003) through development of a relative chronology of structural and metallogenic events.

Since the completion of geological mapping of the West African Craton in the 1980s by the BRGM, geological mapping has been focused in areas with potential mineral deposits including gold deposits in the Ashanti Belt and Tarkwa Basin in Ghana (Milési et al., 1989, 1991; Feybesse et al., 2006). In Burkina Faso studies completed by Feybesse et al. (1990), Lompo et al. (1991, Béziat et al. (2000) and Hein et al. (2004) have focused on the Boromo-Goren Greenstone belt and associated gold mineralization. However, little or no research has been undertaken to develop an understanding of first order crustal scale structures and their relationship to gold mineralization in the Essakane goldfield. This is the purpose of this report.

1.2 Location and physiography

The area of study is located ±250 km NE of the capital city, Ouagadougou, Burkina Faso (Fig. 1). Burkina Faso is a landlocked country in West Africa. The neighbouring countries include Mali, Niger, Benin, Togo, Ghana and Côte d`Ivoire. The official language is French. Other languages, local languages include Mooré and Dioula. Islam is the dominate religion with more than half of the country's population being Muslim, a small group being Christian, with the remainder practicing indigenous African religions. The land surface is defined by alluvial plains, low hills, and sand dunes of the Sahara in the north. The area of study is situated in the margin of the Sahara desert or Sahel region. In this region more than 60% of the land surface is covered by sand. The dominate vegetation is short-tall grass, with less than 10% cover due to trees.

The climate is variable between two seasons, the wet (rainy) and dry season. The harmattan wind (hot and dry) blows from the Sahara desert during the dry season. During this period the day temperatures can peak at 45ºC with night temperatures averaging 30ºC. The harmattan winds collect dust particles from the Sahara desert and, in so doing, considerably reduces visibility during the harmattan season. Consequently field work for this project was completed at the beginning of the dry season before the harmattan wind started.

1.3 Aims and objectives

The aims of this project are:

- To establish the relative timing of structural events for the Markoye fault.
- To understand the tectonic history.
- To establish the spatial and temporal relationship of the various geological features in the region.
- If possible, to fingerprint the timing of gold metallogenesis.

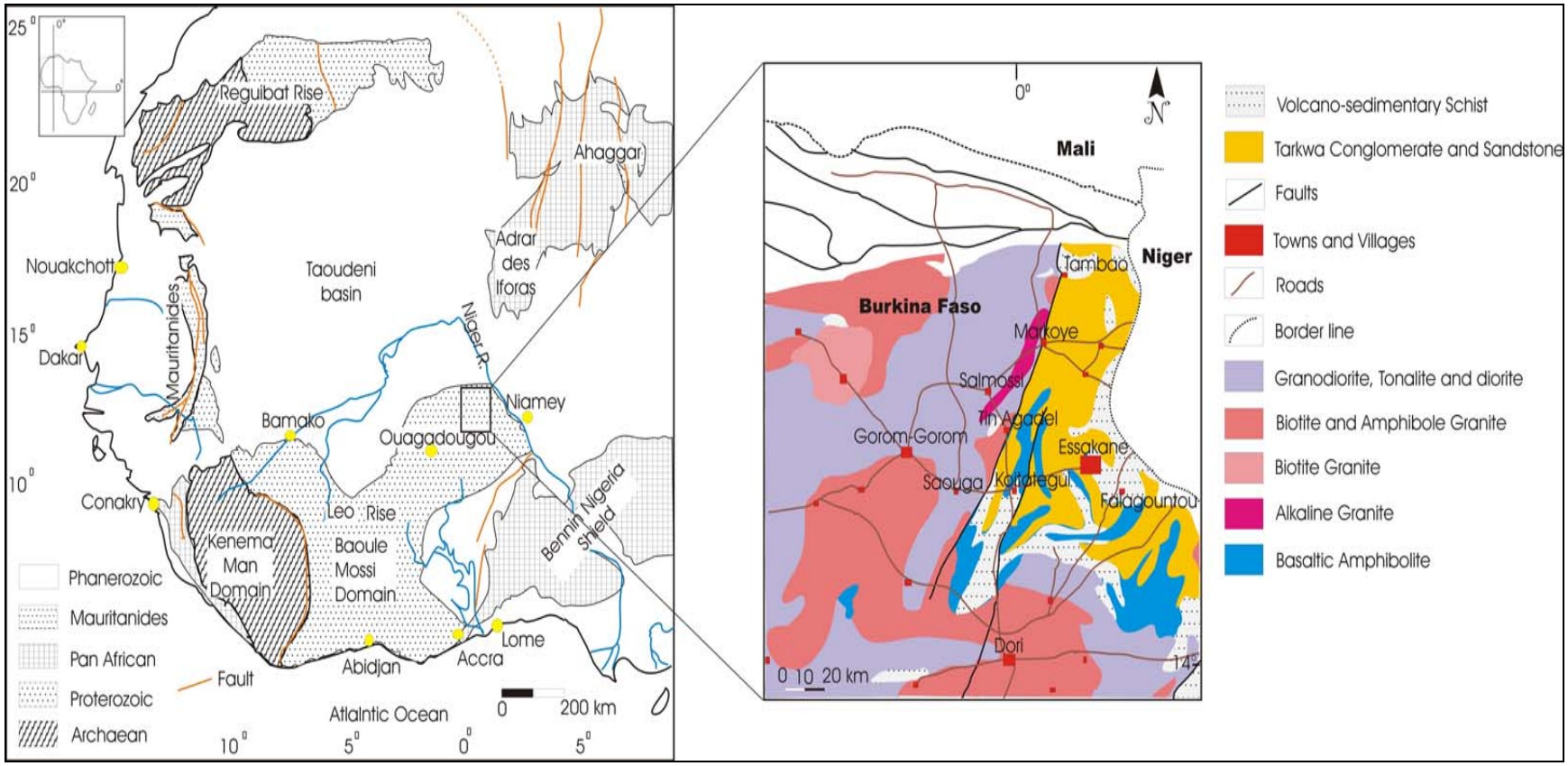

Figure 1. Simplified geological map of the West African Craton after Thièblemont et al. (2004), and the geological map of the study area modified after Castaing et al. (2003). The study area is situated in the Palaeoproterozoic Baoule-Mossi Domain in Burkina Faso.

Chapter 2: Regional Geology

2.1 Preamble

The West African Craton is composed of an Archaean and Palaeoproterozoic basement that is divided into the Reguibat Rise in the north and the Leo-Man Rise in the south (Thiéblemont et al., 2004). These two are separated by the Taoudeni basin, which is of upper Proterozoic to Devonian age (Fig. 1). The Leo-Man Rise is composed of two domains, the Kénéma-Man domain in the south west and the Baoule-Mossi domain in the east (Feybesse et al., 2006). The area of study is situated within the Leo-Man Rise in the Palaeoproterozoic Baoule-Mossi domain. The Kénéma-Man domain is Archaean in age and dated at 3542-3535 Ma (U-Pb zircon, Thiéblemont et al., 2001, 2004). The Baoule-Mossi domain is Palaeoproterozoic in age and consists of Birimian sequences that where accreted at around 2100 Ma during the Eburnean Orogeny (Milési et al., 1991, 1992; Boher et al., 1992). The syn-tectonic emplacement of granitoids during accretion occurred at around 2190-2108 Ma during the Eburnean orogeny (Hirdes and Davis, 2002). The Tarkwa Group which unconformably overlies the Birimian sequences is regarded by some as the erosional product of the Birimian sequences and granitoids (Hastings, 1982; Leube et al., 1990; Milési et al., 1992; Castaing et al., 2003).

2.2 Stratigraphy

The area of study is situated in the NE of Burkina Faso. The overall stratigraphy of the eastern part of Burkina Faso is established by the Palaeoproterozoic basement. The NE-trending Birimian meta-sedimentary and meta-volcanic sequences (2238-2170 Ma) unconformably overlie the basement. The NE-trending Tarkwa Group (2150-2130 Ma) meta-sedimentary sequence overlie the Birimian sequences and they are intruded by Eburnean granitoids (2150-2095 Ma) (Leube et al., 1990; Milési et al., 1991; Bossière et al., 1996; Castaing et al 2003; Naba et al., 2004). Both sequences were deformed during the Eburnean Orogeny at 2100 Ma - 2000 Ma (Milési et al., 1991, 1992; Ledru et al 1994). There is a school of thought that acknowledges a well established unconformity

between the West African Craton and the Birimian sequences (Milési et al., 1989; Davis et al., 1994; Feybesse and Milési., 1994). Furthermore Milési et al. (1992) determined that an unconformity exists between the lower and the upper Birimian series in the type locality in the Goren Greenstone Belt. However Hein et al. (2004) demonstrated that the discordance was structural and that the lower and upper Birimian series are, instead, interbedded. An unconformity also exists between the Birimian sequences and the overlying Tarkwa Group sequences (Leube et al., 1990; Milési et al., 1992; Castaing et al., 2003).

2.3 Birimian sequences

Junner (1935; 1940) in Leube et al. (1990) divided the stratigraphy of the Birimian into two parts. The lower Birimian series (B1) is predominantly sedimentary in origin and includes dacitic/rhyodacitic meta-volcanoclastic sediments, meta-greywacke with intercalated black meta-siltstone and manganiferous chert, argillite, shale and chemical meta-sedimentary rocks (Feybesse et al., 1990; Leube et al., 1990; Hirdes et al., 1996; Milési et al., 1991, 1992). The upper Birimian series (B2) consists of metamorphosed basic (tholeiites pillow lavas and basalts) and intermediate lavas and pyroclastic rocks (Leube et al., 1990; Milési et al., 1991, 1992; Hirdes et al., 1996; Naba et al., 2004). The layout of the Birimian stratigraphy is the subject of controversy. Hirdes et al. (1996) considered B2 to be younger than B1, however, Milési et al. (1991, 1992) and Feybesse and Milési (1994) considered B1 to be younger than B2. In contrast Hein et al. (2004) established that meta-volcanic and meta-pyroclastic units are interbedded with meta-sedimentary rocks throughout the type locality in the Goren Greenstone Belt, and thus the stratigraphy of the NE of Burkina Faso may need revision.

2.4 Intrusive complexes

During the polycyclic Eburnean Orogeny numerous calc-alkaline plutons intruded the Palaeoproterozoic sequences (Pawlig et al., 2006) including tonalite (TTG), granodiorite, diorite and meta-diorite, and these are collectively called Eburnean granitoids (Pons et

al., 1995; Naba et al., 2004; Pawlig et al., 2006). The tecto-magmatic event related to the intrusion of the granitoids is dated at 2200 Ma – 2070 Ma (U-Pb dating) (Liégois et al., 1991). The granitoids cover 50-70% of the Palaeoproterozoic basement of West Africa (Milési et al., 1989; Naba et al., 2004). Two emplacement events have been established (Castaing et al., 2003; Naba et al., 2004). A TTG Suite which is composed of granodiorite, tonalite and quartz-diorite was emplaced between 2210 and 2160 Ma (Castaing et al., 2003). The tonalite suite intrudes and contact metamorphoses the Birimian sequences, and is banded (layered) and foliated in places (Hein et al., 2004; Naba et al., 2004). A granite suite which is localized along shear zones, intrudes both the Birimian and the TTG suite and was emplaced between 2150 and 2130 Ma (Castaing et al., 2003). Gabbro, meta-gabbro, diorite and trondhjemite intrusions are syn-tectonic with emplacement of Birimian meta-volcanic sequences (Béziat et al., 2000; Hein et al., 2004) and co-magmatic (Béziat et al., 2000). NE-trending dolerite dykes crosscut all Birimian, Tarkwa and intrusive complexes in the NE of Burkina Faso and are dated at 250±13 Ma (K-Ar whole rock dating) (Hottin and Ouedraogo, 1992).

2.5 Metamorphism

The Birimian sequences were metamorphosed during the Eburnean Orogeny with further metamorphism related to intrusion of granitoids. Metamorphic grade is to greenschist facies (Milési et al., 1989, 1991; Bossière et al., 1996; Hirdes et al., 1996), with formation of chlorite and muscovite dominant mineral assemblages, and low to medium grade amphibolite facies, with hornblende and andalusite dominant mineral assemblages (Bossière et al., 1996; Béziat et al., 2000; Naba et al., 2004) particularly in the contact aureole of granitoids (Pawlig et al., 2006). The Tarkwa Group is metamorphosed to greenschist facies with development of chlorite and sericite (Milési et al., 1989, 1991).

2.6 Tarkwa Group

The Tarkwa Group is defined from Ghana as clastic meta-sedimentary rocks derived from erosion of the Birimian sequences (Leube et al., 1990; Milési et al., 1991). The

Tarkwa Group unconformably overlies the Birimian sequence (Leube et al., 1990; Milési et al., 1992; Castaing et al., 2003) and was deformed and metamorphosed to greenschist facies during the Eburnean Orogeny (Milési et al., 1989, 1991).

The Tarkwa Group has been divided into three units: the Banket series, phyllite unit and the meta-sandstone unit. The Banket series is further divided into the Banket quartz lithic meta-sandstone unit and the Banket meta-conglomerate unit (Tunks et al., 2004). Kwesie (1984) and Kesse (1985) in Milési et al., (1991) described the meta-conglomerate unit at Tarkwa in Ghana as monomictic, consisting of over 90% rounded vein quartz pebbles and approximately 10 % schist and quartzite pebbles. The matrix is mainly composed of silica and black sands that are rich in heavy minerals including magnetite, ilmenite, rutile and tourmaline (Milési et al., 1989, 1991; Bossière et al., 1996). The Tarkwa Group meta-conglomerate unit hosts and has been the source for economic gold at the Tarkwa mine, Ghana (Milési et al., 1991).

Bossière et al. (1996) established that the metamorphosed sequences of the Tarkwa Group of Burkina Faso (in the study area) were different from those defined in Ghana, in that they contain euhedral zircons that suggest a short transportation distance. In the study area the Tarkwa Group meta-sedimentary rocks are deformed. Their deformation has been attributed to the formation of sinistral shears and low grade metamorphism that is characterised by formation of muscovite (Bossière et al., 1996; Naba et al., 2004), which is similar to what has been defined in Ghana by Milési et al. (1989, 1991). They were divided into 3 main lithological units by Bossière et al. (1996), but the stratigraphic order was not defined. The three main units include: (1) a meta-pelite unit, (2) meta-sandstone unit and (3) a meta-conglomerate unit containing angular clasts of quartzitic and micaceous lithic fragments of rhyolite, chert and schist.

2.7 Structure

Several regional tectono-metamorphic events are recognised in the NE of Burkina Faso. In studies conducted by Feybesse et al. (1990), Lompo et al. (1991), and Hein et al.

(2004) in the Boromo-Goren Greenstone Belt, four deformational events are currently recognised. D1, represented by isoclinal folds (F1) which are synchronous with development of foliation. D2, represented by formation of N, NE and NW-trending sinistral faults that are synchronous with low-grade metamorphism. D3 is represented by NE-trending dextral or dextral reverse faults, also synchronous with low-grade metamorphism. D3 event is associated with the development F3 folds during E-W crustal shortening. D4, which is represented by NW-trending Wabi-Tampelse Shear Zone which crosscuts the Goren Greenstone Belt is associated with development of mesoscopic folds (F4) during N-S crustal shortening (Hein et al., 2004).

2.8 Markoye Fault

The first-order crustal-scale Markoye fault is located in the NE of Burkina Faso, west of the international border intersection of Burkina Faso, Mali and Niger (Fig.1). The fault trends NE and is clearly visible in LANDSAT imagery (Fig. 2) and RTP magnetic data. According to Milési et al. (1989, 1992) and Castaing et al. (2003) the Markoye fault is the boundary that separates Eburnean granitoids to the west from the Tarkwa Group meta-sedimentary units in the east. In Milési et al. (1989, 1991, 1992) and Hottin and Ouedraogo (1992), the Markoye fault is recorded as a westerly-dipping thrust but field data was not presented. Unpublished structural studies completed for Goldfields Mining Pty, Ltd, Ore Zone Resources and BHP Billiton concluded that the Markoye fault is an east-verging thrust (Rogers and Dong, 2000) and that it is a part of a regional dextral strike-slip system.

2.9 Regional metallogeny

The West African Craton hosts many mineral deposits, for example, gold, diamond, iron, and manganese, silver, lead and zinc (Hastings, 1982; Milési et al., 1992). Several deposits and deposit styles occur in the study area including; (1) The manganese deposit at Tambăo close to border with Niger (Fig. 2), (2) gold mineralization at Essakane, Gosséy, Koiréziéna, Falagountou (Fig. 2) and Sebba (Milési et al., 1992; Castaing et al.,

2003), and (3) pegmatites veins bearing tourmaline plagioclase and topaz crystals near Tambăo. Several deposits are associated with the sulphidised brittle-ductile shear zones, including gold in sheeted and stockwork quartz veins, copper as malachite in buck quartz veins, and tourmaline and topaz in pegmatite and buck quartz veins (Foster and Piper, 1993; Lompo, 2001; Castaing et al., 2003). Foster and Piper (1993) have restricted gold mineralization of the West African Craton to the Eburnean tectonothermal event, but this does not include gold hosted by the Tarkwa Group meta-sedimentary units in Ghana (Milési et al., 1991; Feybesse et al., 2006) which formed after the Eburnean event. Bossière et al. (1996) concluded that the Tarkwa Group meta-sedimentary units in the study area have no economic value.

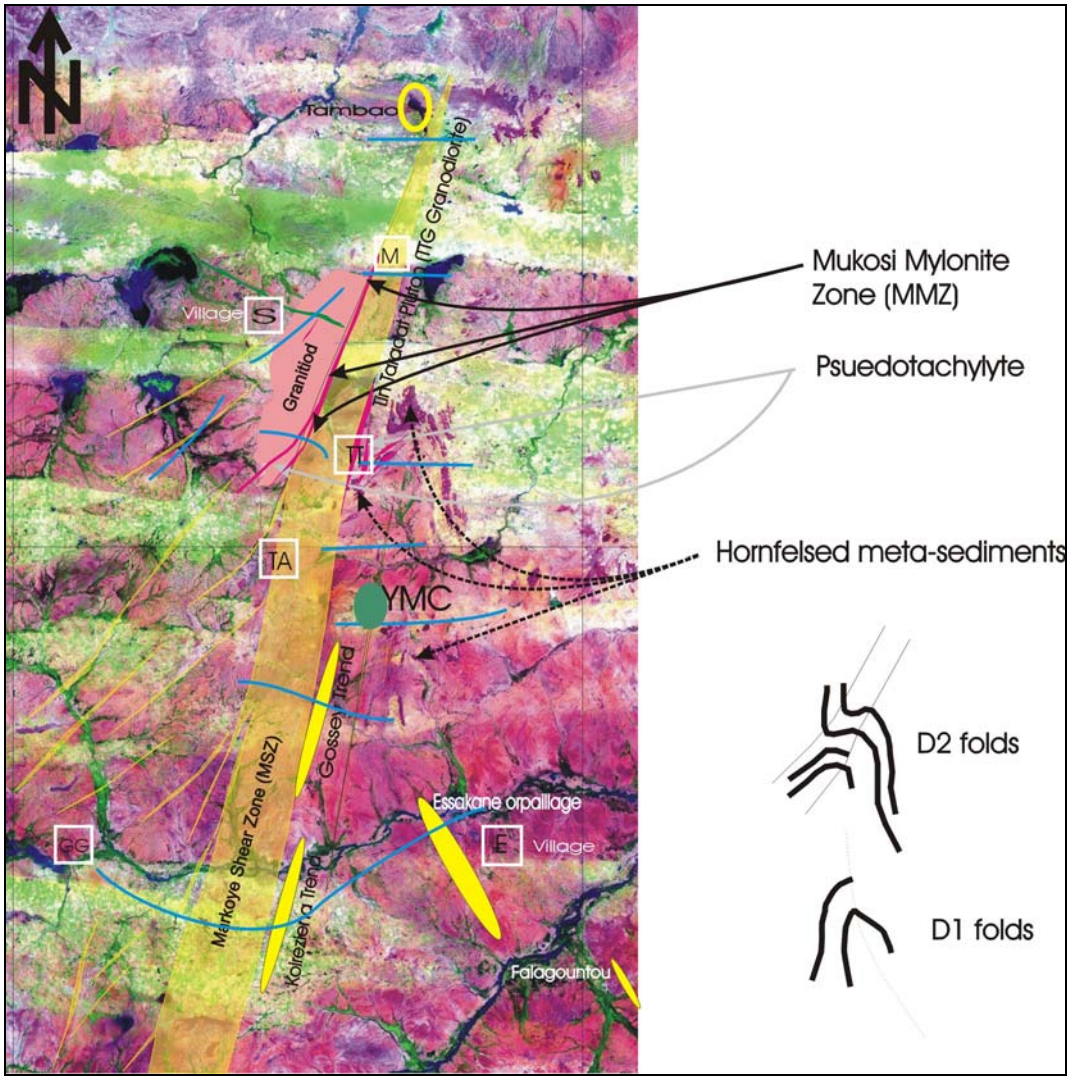

Figure 2. Schematic interpretation of LANDSAT image, modified after Hein and Tshibubudze, 2007 showing locations of villages, orpaillage ( ) and traverse lines ( ). The villages are: Salmossi (S), Essakane (E), Tin Agadel (TA), Tin Taradat (TT), Markoye (M), and Gorom-Gorom (GG). The (YMC) Yacouba Mafic Complex .

Chapter 3: Methodology

3.1 Data collection

In January 2007 a detailed structural mapping project was conducted in the study area over a period of 20 days, including days allocated to logistics and camp management. Geology and topographic maps, and airborne magnetic data were used to delineate the Markoye fault. Geographic and geologic reconnaissance studies of the region were conducted before the actual field work commenced. Several east-west traverses were conducted across the Markoye fault between Essakane and Tambăo (Fig.1 and 2). For each station point mapped, lithological and structural data was recorded, a photographic record was made, GPS position was established using UTM grid co-ordinates (WGS 84), and if appropriate, samples were collected for petrographic studies.

The data was captured using a northern hemisphere compass clinometer, and the geographic coordinates were recorded using Garmin Geographic Positioning System (GPS) instrument. A geological hammer was used for sampling. Digital camera was used for photograph, and a handlens for mineral identification. For most of the outcrops, stratigraphic facing was established from primary sedimentary features including bed gradation, scour and fill, cross-bedding, ripple marks, etc. In areas of limited outcrop, with a cover of ferricrete or alluvium, sub-crop geology mapping was used to provide qualitative stratigraphic data.

Both oriented and non-oriented samples were collected to assist with lithological descriptions and future micro-structural analysis in 2008. Samples where labelled, described and bagged. All samples where transported to Orezone Resources main office in Ouagadougou, and then transported to Johannesburg by Air France flight. Samples were catalogued and submitted to SGS laboratories in Booysens Johannesburg to make polished thin sections (PTS). Oriented samples were referenced to magnetic north, and marked with horizontal and vertical orientation lines.

3.2 Data processing and interpretation

An Excel (Microsoft) spreadsheet was created to catalogue structural elements and lithological descriptions. The spreadsheet is presented in Appendix A. Corel DRAW 9.0 was used for drawing maps and diagrams. GEORIENT 9.2 (Holcombe, 2006) was used to analyse structural data.

Chapter 4: Lithologies

4.1 Preamble

The lithologies of the study area consist of metamorphosed volcano-sedimentary and sedimentary sequences. These sequences have been intruded by plutonic rocks that include granodiorite-tonalite, pyroxenite-gabbro, granite (adamellite) plutons and dolerite dykes. The plutons and dyke have contact metamorphosed the rocks of the region to hornblende-hornfels facies (Fig. 2). All the lithologies in the area have been subjected to several phases of local-regional deformation, with development of schistosity (shearing), mylonite-ultra-mylonite, cataclasite, and L-tectonite (Chapter 5). The lithologies are capped by laterite and alluvium-dune sand profile in places.

4.2 Greywacke-Siltstone sequence

The sequence is metamorphosed and it is magnetic in places. Sedimentary structures are preserved as compositional layering in the contact aureole of intrusions. Facing direction is east as determined from graded bedding, and scour and fill. The general orientation of foliation (cleavage) is north-east trending. The general orientation of bedding is north-north-east trending. Crosscutting quartz veins are generally orientated north-east.

The monotonous greywacke-siltstone sequences at the Essakane orpaillage west of the Essakane village (Fig. 2) hosts crosscutting quartz-carbonate veins, and gold-arsenopyrite mineralization is hosted in the alteration zone surrounding the quartz-carbonate veins in competent greywacke sandstone units. The greywacke-siltstone sequence has been folded. Siltstone units are spotted with ovoid porphyroblasts of cordierite (thermally metamorphosed). Siltstone, greywacke, sandstone and shale layers are interbedded. Shale is dark-grey to black in colour, and contains a pronounced pencil cleavage. Stromatolites occur in siltstone-sandstone sequences (Fig. 3) south of the Gosséy trend (Fig. 2).

West of the Essakane orpaillage (Fig. 2) the lithologies are dominated by greywacke sandstone that contains shale fragments. Primary sedimentary features including sand-balls, slumps and cross-bedding are preserved as compositional layering. The pebble lag at the bottom of the greywacke sandstone layer is polymictic with clasts of shale (black) and chert. The sequences have been contact metamorphosed to hornblende-hornfels facies by a mafic dyke intrusion.

4.3 Massive volcanoclastic greywacke sequences

Massive volcanoclastic greywacke units underlie the greywacke siltstone sequences, and are predominantly composed of quartz and feldspar grains in a fine to medium grained matrix (Fig. 4, d). Facing is to the east, as determined from cross beds, scour and fill, ripple marks, laminations, slumps, mud-balls, sand-balls, and graded beds (Fig. 4, a, b, and c). Fuchsite layers (Cr-muscovite, Navas et al., 2004) (Fig. 4, a) and mud-cracks occur in some meta-volcanoclastic beds. The mud-cracks indicate shallow marine or tidal environment.

4.4 Conglomerate

Conglomerate units are polymictic and matrix supported. They are composed of boulders of granite, granodiorite, gabbro, chert, quartz veins, andesite, basalt and volcanoclastic sedimentary rocks, in a greenish, fine to coarse grained poorly sorted volcanoclastic matrix (Fig. 5, a, and b). The clasts are sub-rounded to angular and up to 30cm in size (Fig. 5, a, and b).

4.5 Laterite

Laterite is iron-rich profile that is developed under tropical to sub-tropical condition due to long term exposure of rocks to the atmosphere and hydrosphere in tectonically stable areas (Dequincey et al., 2006). In an isotopic study conducted across the West African Craton, using ^{10}Be and ^{26}Al isotopic depletion ratios of laterite, Brown et al. (1994)

concluded that in-situ laterite in Burkina Faso formed during the upper Cretaceous to Eocene. The laterite is randomly distributed in the northern part of the study area.

4.6 Alluvial profile

The alluvial profile in the area of study is dominated by light coloured, fine to medium sand with fragments of siltstone and quartz-vein material. The alluvial profile covers most of the landscape in Burkina Faso.

4.7 Intrusions

4.7.1 Biotite Granite/ Adamellite

A biotite granite/adamellite crops out west of the Markoye fault (Fig. 2). It is medium to coarse, and composed of millimetre-sized crystals of potassium feldspar, quartz, plagioclase, biotite and hornblende in a quartz-feldspar rich groundmass (Fig. 6, a, b and c). Adjacent to the Markoye fault the granite is foliated and lineated.

4.7.2 Yacouba Mafic Complex (YMC)

The YMC is located NE of the Gosséy orpaillage (Fig. 2). It is composed of pyroxenite and gabbro layers. The gabbro is coarse, light coloured, and composed of large crystals of plagioclase, quartz and pyroxene (Fig. 7, a, b). It is NE-trending with numerous gabbro dykes that radiate away from the main intrusion. The dykes predominantly trend NW.

The pyroxenite layer consists of large (>1cm) pyroxene and olivine crystals in a pyroxene-olivine-nepheline groundmass (Fig. 8, a, b). The intrusion constites a mafic layered suite that is differentiated with gabbro-norite layer. The gabbro-norite layer hosts lithic xenoliths, and is crosscut by quartz veins. The contact aureole to the intrusion hosts spider-type veins and contraction fractures due to cooling of the intrusion. The pyroxenite

is crosscut by a week anastomosing cleavage that is non penetrative. The cleavage crosscuts post-dates the emplacement of pyroxenite intrusion.

NW-trending pyroxenite dykes are composed entirely of pyroxene crystals and hornblende. The wall rocks to these dykes are contact metamorphosed to hornblende-hornfels facies.

4.7.3 Granodiorite-Tonalite

A granodiorite-tonalite intrusion outcrops over greater than 50% of the study area west of the Markoye fault between Gosséy and Tambão (Fig. 1). The granodiorite-tonalite pluton is coarse to medium, and composed of crystals of plagioclase, quartz, hornblende and biotite (Fig. 9). It is crosscut by pseudotachylyte veins west of the Markoye fault. It hosts elongate mafic xenoliths that trend NW and dips to the west. The hereafter referred to as the Tin-Taradat granodiorite-tonalite (Fig. 2) is crosscut by a pegmatite vein. The pegmatite vein is ±40 cm thick, and it trends NE. It is a plagioclase-tourmaline-topaz pegmatite with crystals greater than 10cm in size.

4.7.4 Dolerite

A series of parallel NW-trending, mafic magnetic dolerite dykes crosscut the study area. They are composed of plagioclase, clinopyroxene and magnetite and commonly exhibit granophyric texture in thin section. The mineralogical composition is given in Figure 10. The dykes crosscut greywacke-siltstone sequences at the Essakane goldfield and have contact metamorphosed these sequences to hornblende-hornfels facies. The contact aureole rocks of these dykes are strongly magnetic.

Figure 3. Stromatolites in a sandstone outcrop south of Gosséy. Compass clinometer for scale. GPS, N 14 26 22 3 W 00 00 16 3.

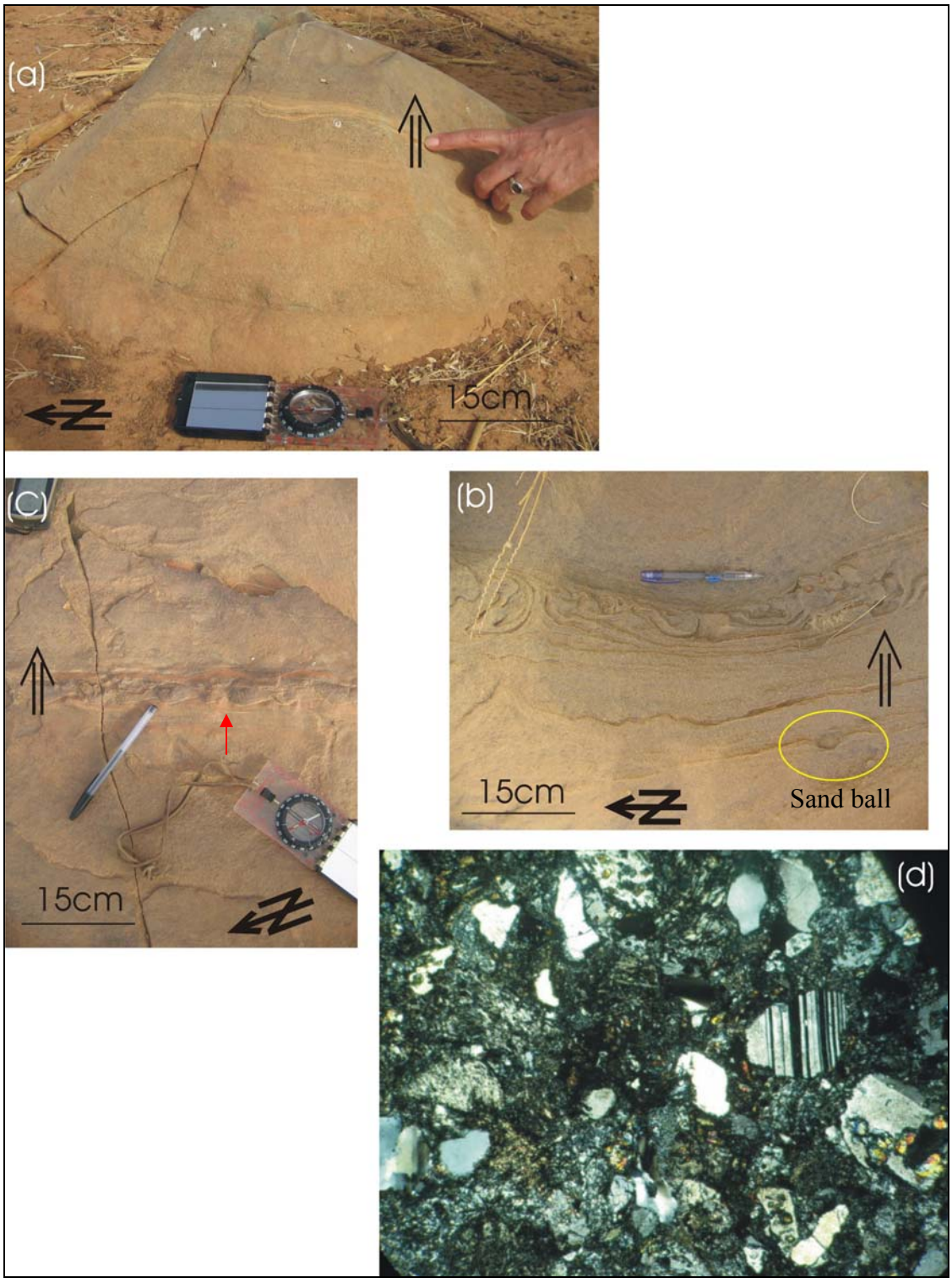

Figure 4. (a) Contact metamorphosed meta-volcanoclastic greywacke east of the Markoye fault showing bed layering compositional and interbedded fuchsite layer. GPS, N 14 38 30 7 E 00 03 36 2. (b) Slump flow and sand-balls preserved in a meta-greywacke

sequence west of Essakane. GPS, 0184836- 1587581 (c) Preserved primary sedimentary structure, ripple marks above the red arrow head and sour and fill texture. GPS, N 14 38 03 3 E 00 03 32 8. The arrows indicates the facing direction (d) Photomicrograph (plane polarised light, X4 magnification), of meta-volcanoclastic greywacke (sample 005). The greywacke is poorly sorted and contains rock fragments, anhedral quartz, plagioclase grains, and isotropic minerals in a fine to medium grained quartz-feldspar-chlorite matrix.

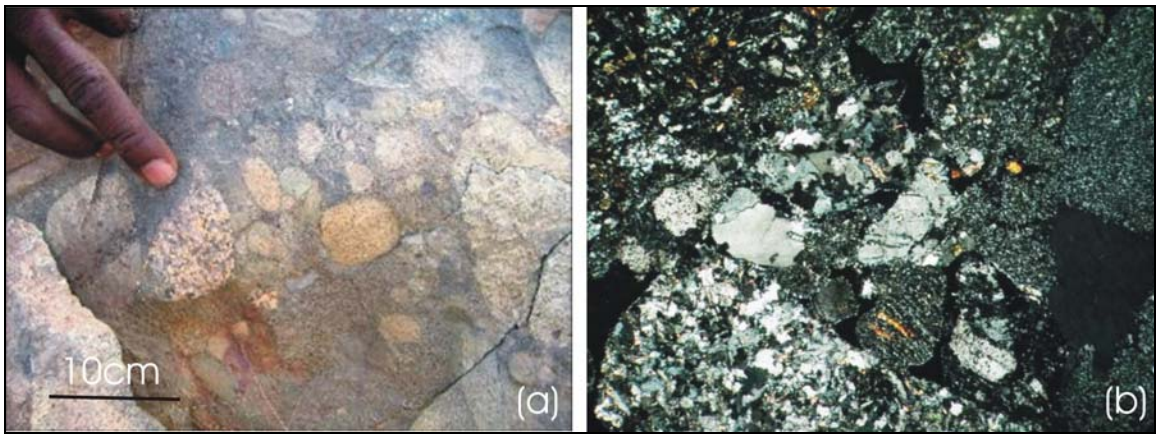

Figure 5. (a). The polymictic, matrix supported conglomerate unit in the study area. GPS, N 16 19 70 0 E 01 82 69 1 (b) Photomicrograph of the matrix of (a) under plane polarised light (X4 magnification). The matrix is poorly sorted and composed of single and polycrystalline quartz, plagioclase, chlorite and fine to coarse grained rock fragments.

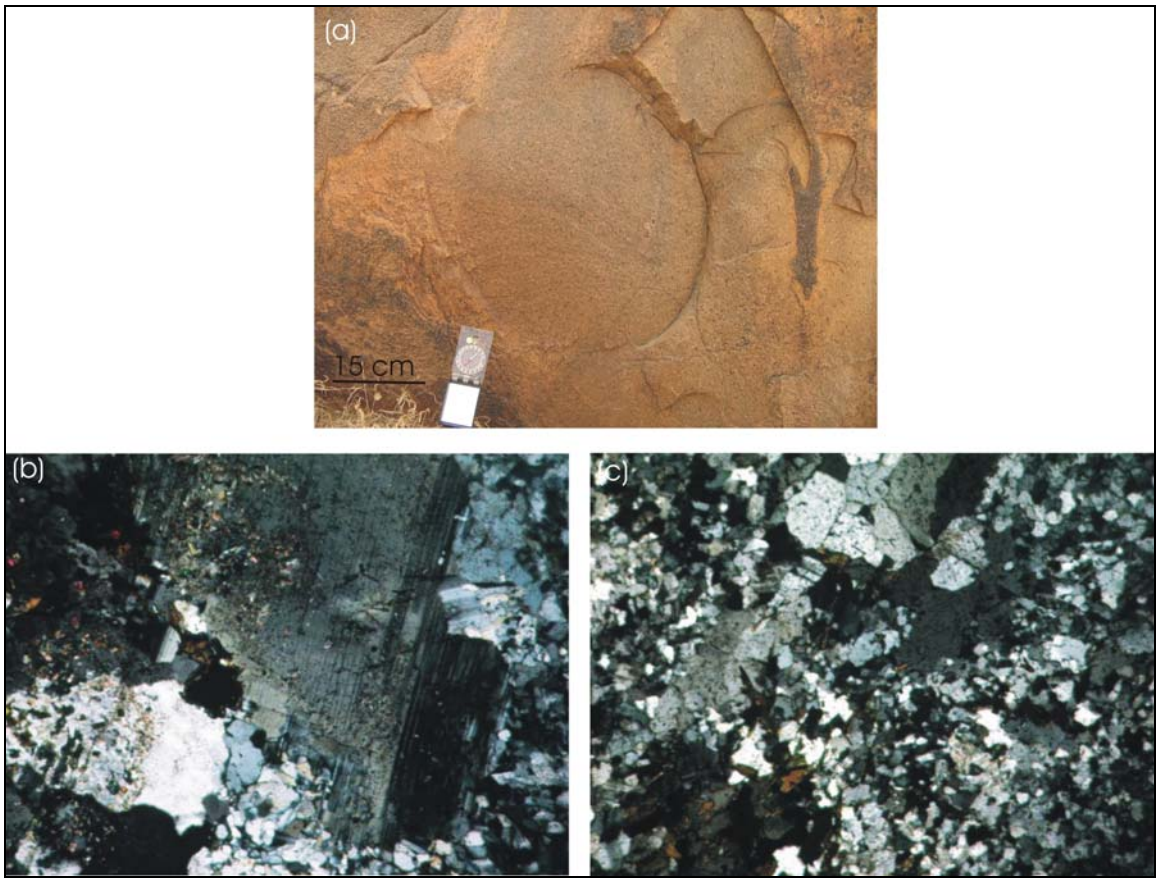

Figure 6. (a) The adamellite which crops out west of the Markoye fault. GPS, N 14 36 31 8 W 00 00 45 2. (b) Photomicrograph of adamellite. The adamellite is K-feldspar dominant. Phenocrysts of plagioclase in a quartzitic-feldspar matrix are partially re-crystallized. (c) Polycrystalline quartz (undulating extinction) crystals and biotite with few crystals of muscovite.

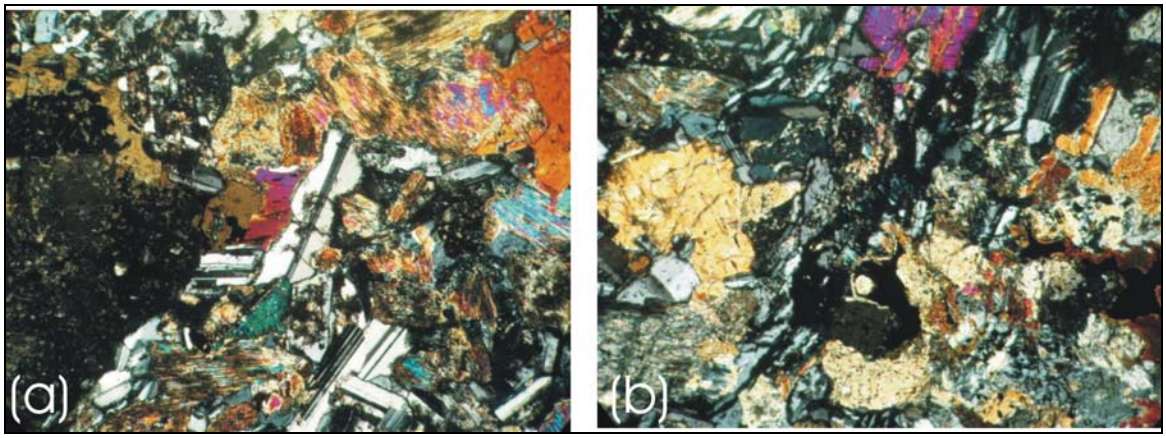

Figure 7. Photomicrographs of a gabbro (X 4 magnification) under plane polarised light. This gabbro is composed of euhedral plagioclase, amphibole, clinopyroxene, biotite, and isotropic minerals (sulphides).

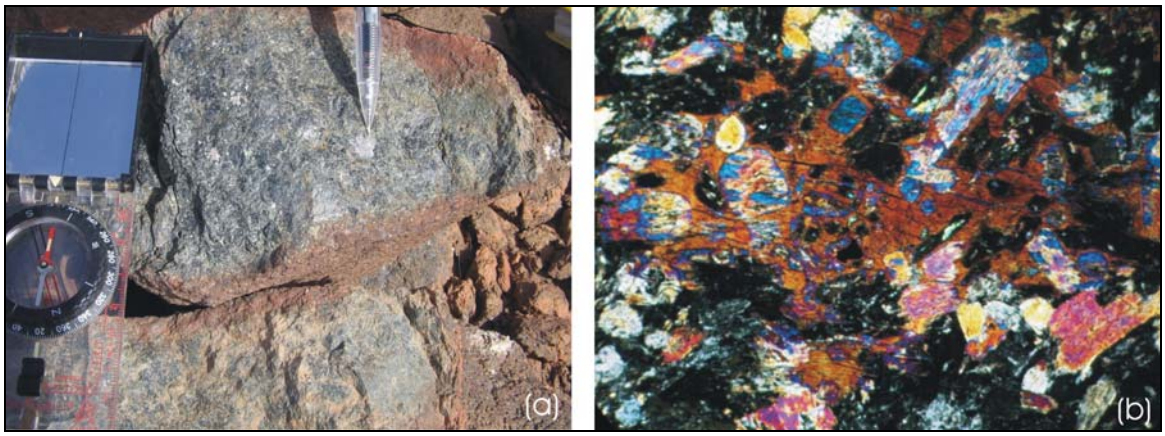

Figure 8. (a) The pyroxenite layer of the YMC. GPS N 14 30 27 7 E 00 00 16 2. (b) Photomicrograph of crystals of clinopyroxene and nepheline of the pyroxenite layer of the YMC.

Figure 9. Coarse to medium granodiorite-tonalite, which is composed of plagioclase, quartz, hornblende and biotite crystals. The nature of banding that is parallel to strike of the compass clinometer is not known. GPS 14 35 05 7 W 00 00 05 4.

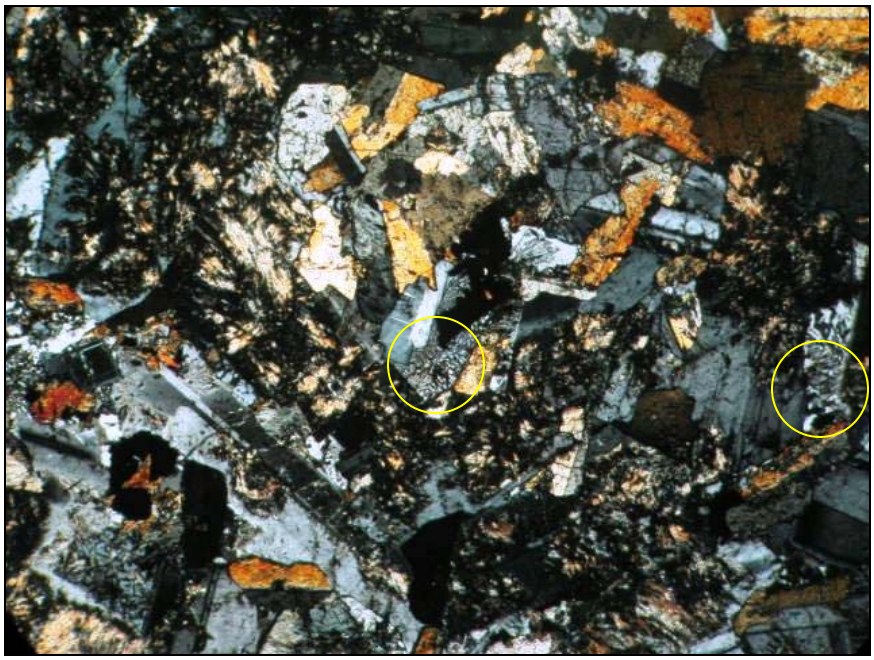

Figure 10. Photomicrograph of dolerite (X 4 magnification) under plane polarised light. This dolerite is composed of crystals of plagioclase, clinopyroxene and mignetite. Intergrowths of quartz and alkali-feldspar (granophyric texture) are common (yellow rings).

Chapter 5: Structure

5.1 Preamble

The Markoye fault is ~5 km wide and is NE-trending. It is a composite structure of faults, shears, L-tectonites, zones of mylonitisation and pseudotachylyte veins. It hosts an en echelon buck quartz-carbonate vein array. The structure has undergone two phases of brittle-ductile deformation and at least two phases of reactivation are recognised. D1 resulted in the development of the NW-trending asymmetric fold (F1), and the sense of displacement on the Markoye fault was dextral (reverse). D2 marked a period of sinistral (reverse) displacement on the Markoye fault with refolding of F1 to form NE-trending folds (F2). F1 and F2 are crosscut by faults and quartz-chlorite shears associated with the development of quartz-carbonate veins during reactivation of the Markoye fault.

5.2 D1

D1 is associated with the formation of NW-trending folds (F1) that are clearly evident in the exploration trenches at Essakane Orpaillage (Fig. 11). An equal area projection of the poles to bedding exposed in the trenches in the southern part of the Essakane Orpaillage is presented in Figure 12. The mean strike and dip is 343°/27°E. Calculated fold axes plunge 2° towards 348°. Folds are upright, open and asymmetric. Beds facing in both limbs were determined from scour and fill, graded beds, and laminations. A pervasive cleavage is not evident in the trenches, but this could be due to the weathered nature of the meta-sedimentary units.

Rogers and Dong (2000) concluded that a series of north-east dipping thrusts also formed during fold formation. In summary the data suggest that the tectonic transport during formation of F1 and thrusts was to the SW. F1 is crosscut by stockwork, breccia quartz-carbonate veins. An east dipping strike-slip fault transects the anticline, late strike-slip faults are also described by Delisle (2003).

5.3 D2

The second deformation event (D2) is marked by the period of SE-NW crustal shortening during which NE-trending structures were developed. These structures include folds (F2), a zone of mylonite to ultra-mylonite herein referred to as Mukosi Mylonite Zone (MMZ), pseudotachylyte veins, buck quartz-carbonate (± tourmaline) veins, cataclasite, quartz-chlorite shears and L-S tectonites. This phase marks a period of sinistral (reverse) displacement along the Markoye fault.

The meta-sedimentary units east of the MMZ are folded about NE-trending fold axes (F2) as is evident from LANDSAT imagery (Fig. 2). F2 folds are tight and asymmetric. They are crosscut by the MMZ.

The Mukosi Mylonite Zone (MMZ) crops out east of Salmossi village (Fig. 2). The MMZ is NE-trending. This zone is defined by mylonitised to ultra-mylonitised meta-sedimentary rocks and granitoids. The MMZ is a planar, banded, corridor of fine grained rock with a well developed mylonitic fabric, and numerous σ and δ clasts and rotated porphyroclasts. The sky-blue sigmoidal porphyroclasts (cordierite) are hosted in a fine grained dark-blue-grey coloured matrix (Fig. 13). There are well developed shear bands, meso-isoclinal and asymmetric flow folds (Fig. 14 and 15 respectively). The MMZ hosts a penetrative mylonitic foliation and a well developed vertical stretching lineation that is NE-trending. Stretching lineation in granitoid rocks is defined by the mineral hornblende.

Two zones were defined: (1) steeply dipping mylonite foliation and zones of boudinage in which stretching lineation was vertical (Fig.16) which were bounded by (2) steeply dipping corridors of mylonite foliation in which stretching lineation was horizontal (Fig. 16). The poles to the mylonite foliation are vertical and this is well illustrated in Figure 16. The MMZ is interpreted as a high strain zone which represents the ductile deformation phase of D2. The MMZ crosscuts the meta-sedimentary units and the granitoid.

In Figure 16 the stereographic projections of the lineation and schematic structural model shows the extension direction relative to the principal compressive stress. The sense of movement is interpreted from the K-feldspar fish structure, and σ and δ clasts. The σ clasts indicate a sinistral (reverse) displacement (Fig. 16). The MMZ is crosscut by meso-faults and quartz-chlorite shears. The quartz-chlorite shears are mineralized.

Pseudotachylyte veins in the area are represented by very fine grained glassy textured, dark-grey to black glass that fill fractures and meso-faults in the host rocks. They are several centimetres thick (Fig. 17, a, b). They outcrop in the region between Tin Agadel and Salmossi village (Fig. 2) and they crosscut the adamellite and the granodiorite-tonalite intrusion (Fig.17, a, b) north-east of Tin Agadel. The pseudotachylyte veins are NNE-trending and steeply dipping to the east. The pseudotachylyte veins are interpreted to have formed during high strain conditions, the resulting frictional heat melting the host rock (Davis and Reynolds, 1996).

Quartz iron-rich cataclasite veins (Fig. 18, a, b, c) outcrops west of the Yacouba Mafic Complex (YMC) (Fig.2). The cataclasite veins trends 067º and crosscut the YMC. The cataclasite veins are interpreted to have formed during local dilation of the Markoye fault. Quartz-chlorite shear crosscut the cataclasite and the YMC as well indicating that the quartz-chlorite shears are younger than the YMC and the cataclasite.

Buck quartz-carbonate (± tourmaline) veins outcrop in several locations along the trend of the Markoye fault. They are white to brown in colour but in some outcrop they are dark grey and hosted by quartz-chlorite schist. They have an average size of 100 X 5m (Fig. 19) and veins form an en echelon array indicating a sinistral normal displacement. They host centimetre-sized arsenopyrite ($AsFeS_2$) crystals and copper oxide in form of malachite ($Cu_2CO_3(OH)_2$). Some buck quartz-carbonate veins are highly fractured, boudinaged and lineated, producing an egg box textured outcrop (Fig. 19). The stretching lineation plunges steeply with a mean of 68º towards 162° (Fig. 20).

The quartz-chlorite shears are NE-trending. The schitosity measurements are represented in Figure 21. Schistosity crosscuts the YMC and MMZ. The anastomosing cleavage is developed at the edge of YMC.

5.4 Relative chronology of structural events

- Formation of NW-trending folds (F1) and thrusts during SW-directed compression with dextral reverse movement on the Markoye fault.
- Formation of NE-trending folds (F2) during SE-NW compression with sinistral (reverse) displacement on the Markoye fault with development of mylonite zone (MMZ) and pseudotachylyte veins and quartz iron-rich cataclasite veins.
- Formation of quartz-chlorite shears which host buck-quartz carbonate (± tourmaline), stockwork, and breccia veins. The veins are associated with sulphide ± gold mineralization.

5.5 Markoye Fault versus Markoye Shear Zone (MSZ)

Markoye fault is defined by ductile (mylonitised meta-sedimentary rocks and granitoid rocks) deformation, with the development of regional mylonite foliation and schistosity. The Markoye fault is ~5 km wide, and is a composed of numerous faults and shears. The shears are well defined by development of C-S foliation, en echelon quartz-carbonate (± tourmaline) veins, and mineral, stretching and slickenfibre lineation. Hence it is not a fault in the strict sense of the term. It is therefore suggested that it be renamed as a shear zone, the Markoye Shear Zone (MSZ).

Figure 11. Photographic mosaic of Essakane exploration trench number 1. This trench wall is southeast facing, and the pictures were taken facing to the northwest. The Essakane prospect is hosted by an asymmetric open anticline. The stockwork, breccia, and sheeted quartz-carbonate veins are concentrated (hosted) in the eastern limb, the west-dipping cavities on the NE limb where produced by orpailleurs who excluded west-dipping, gold bearing veins.

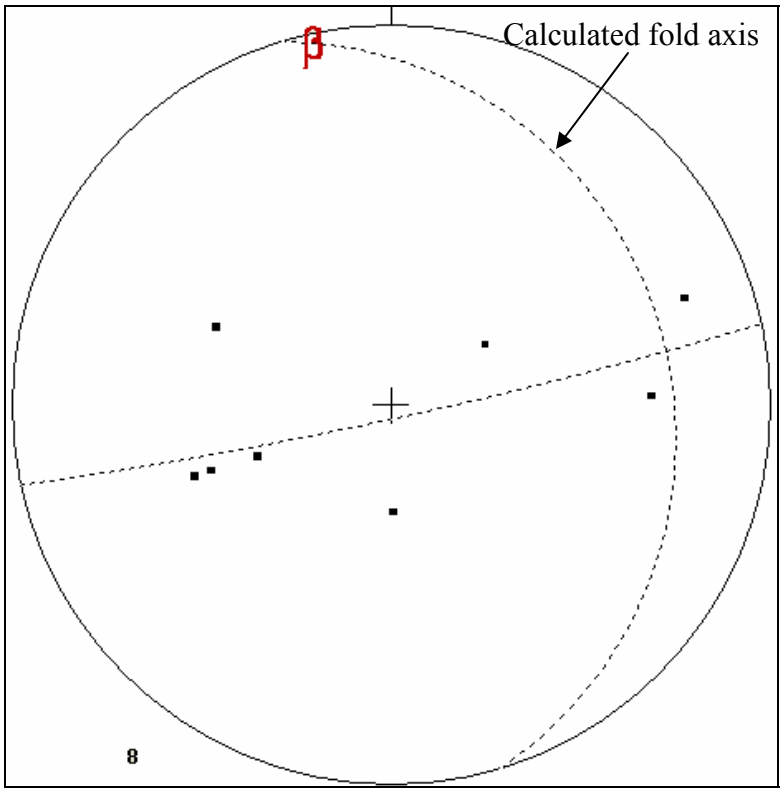

Figure 12. Equal area stereographic projection of the poles to bedding at Essakane exploration trenches. The calculated mean strike and dip is 343°/27°E. The calculated best fit girdle is 078°/88°S. The spread of the poles along the girdle indicates that the bedding has been folded; the calculated mean strike and dip is inferred to parallel the fold axes. The fold is asymmetric with the fold vergence to the SW indicating that the transport direction is toward the SW.

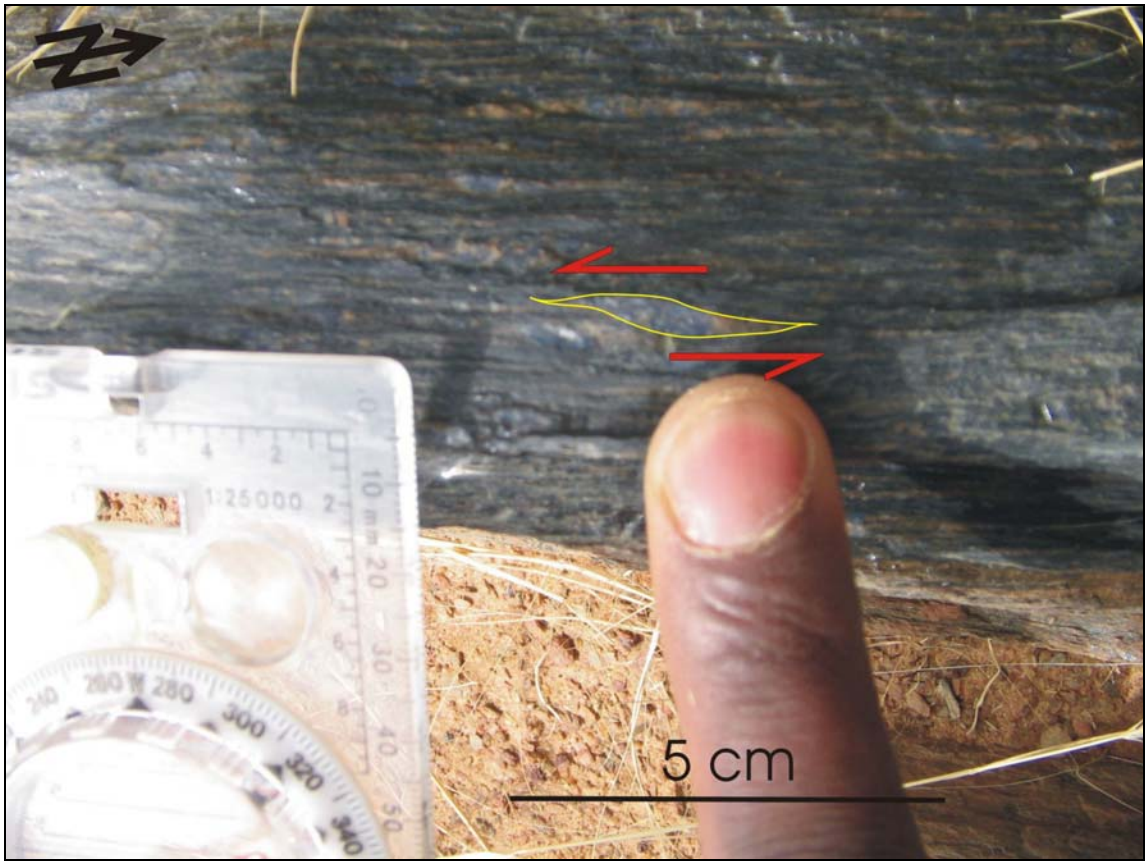

Figure 13. Mylonite hosting sigmoidal porphyroclasts of cordierite in a fine grained dark-blue-grey coloured matrix. The sigmoidal porphyroclasts indicate sinistral displacement. GPS, N 14 36 43 9 E 00 00 01 4.

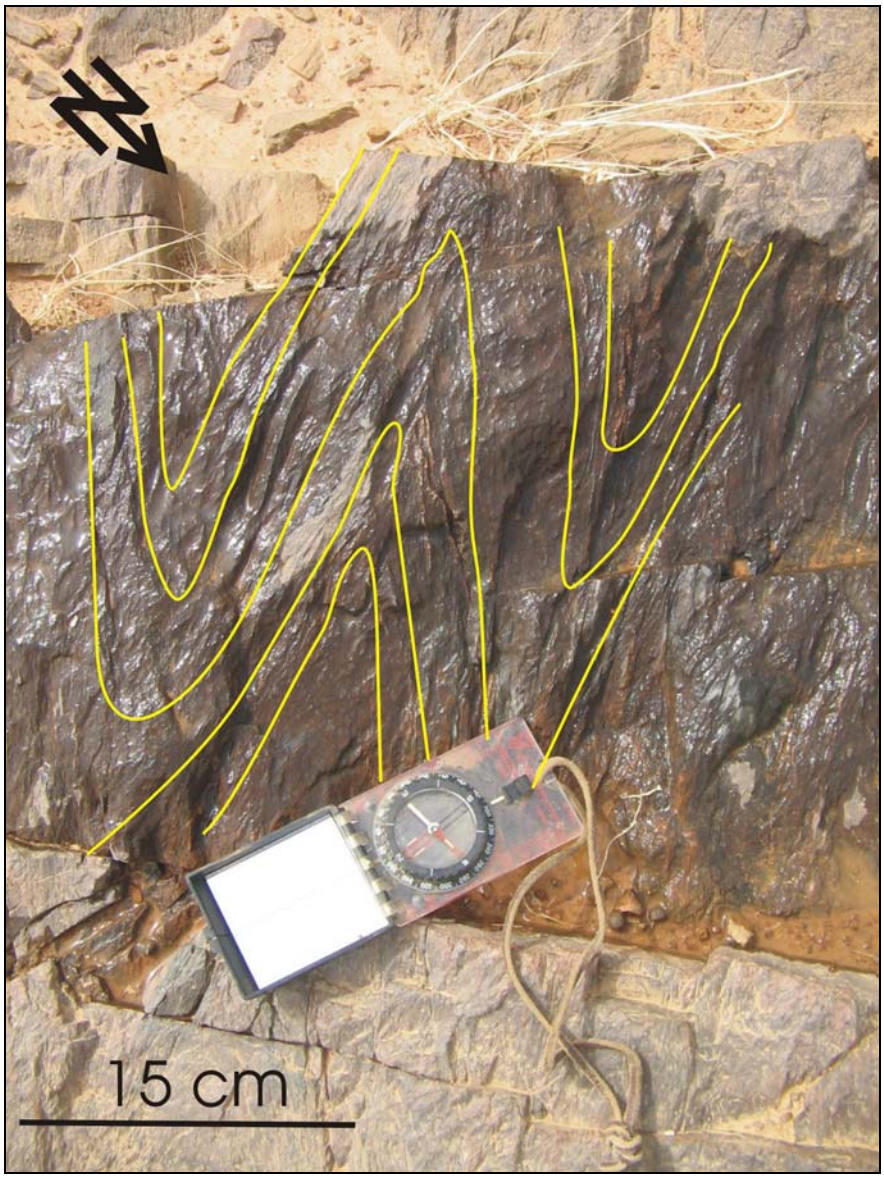

Figure 14. Meso-isoclinal folds in the MMZ. GPS, N 14 36 39 4 E 00 00 10 4.

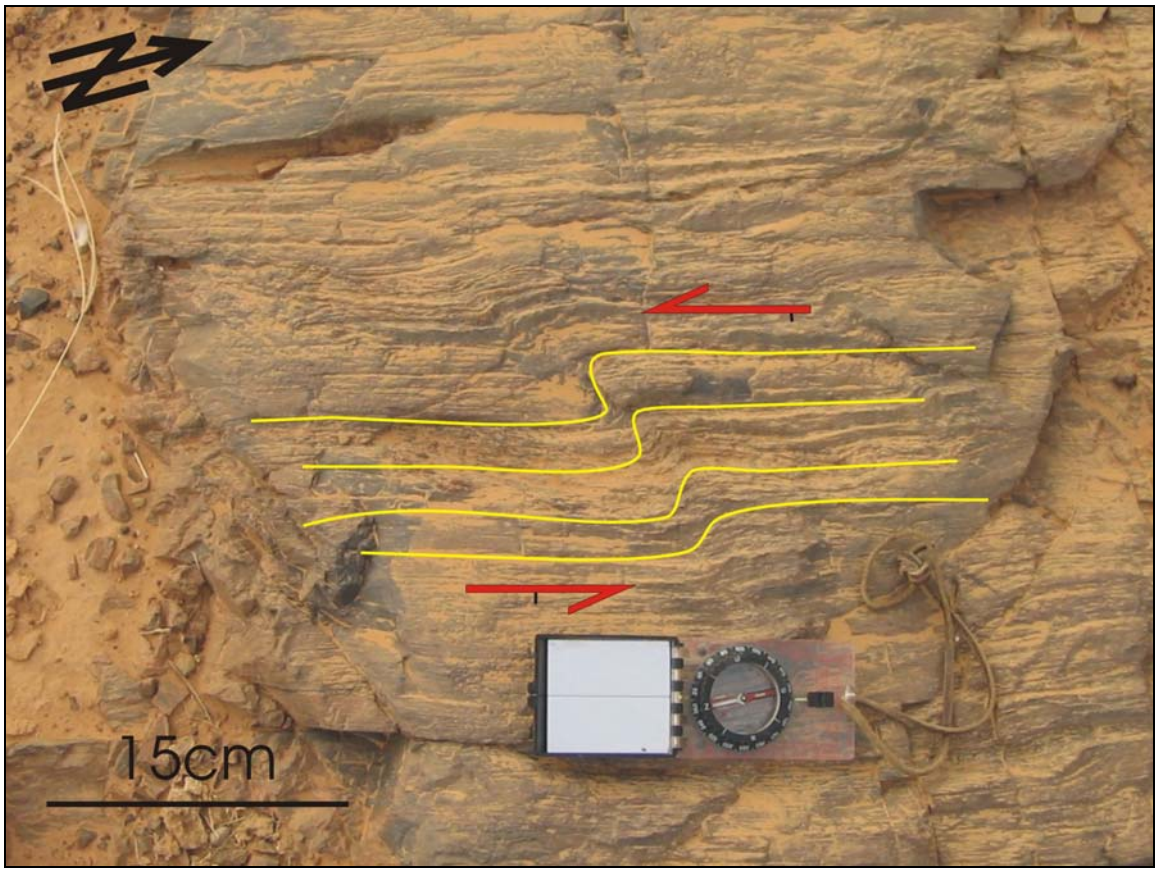

Figure 15. Mylonite with well developed asymmetric flow folds that developed during a sinistral displacement on the MMZ. The folds are synchronous with the horizontal stretching lineation. GPS, 14 36 37 8 E 00 00 12 1.

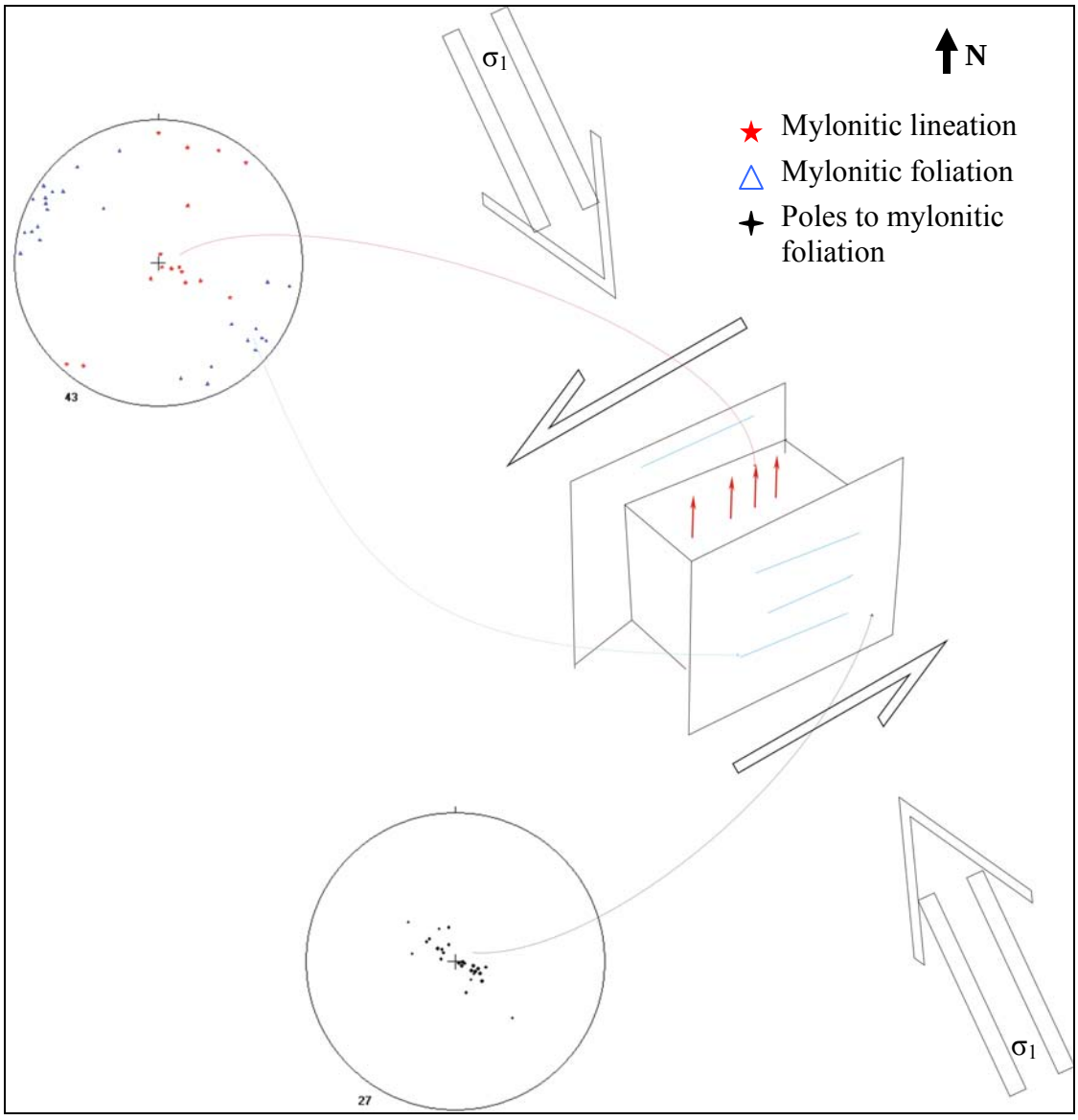

Figure 16. Equal area stereographic projections of mineral and stretching lineation, and foliation in mylonite. The calculated mean principal direction is 73° towards 056° for lineation. The lineation lie on the calculated great circle orientated 025°/81°E. The poles in the middle of the great circle show vertical stretch and the poles in the sides shows horizontal stretching parallel to foliation. The model is illustrating the strain partitioning in the MMZ.

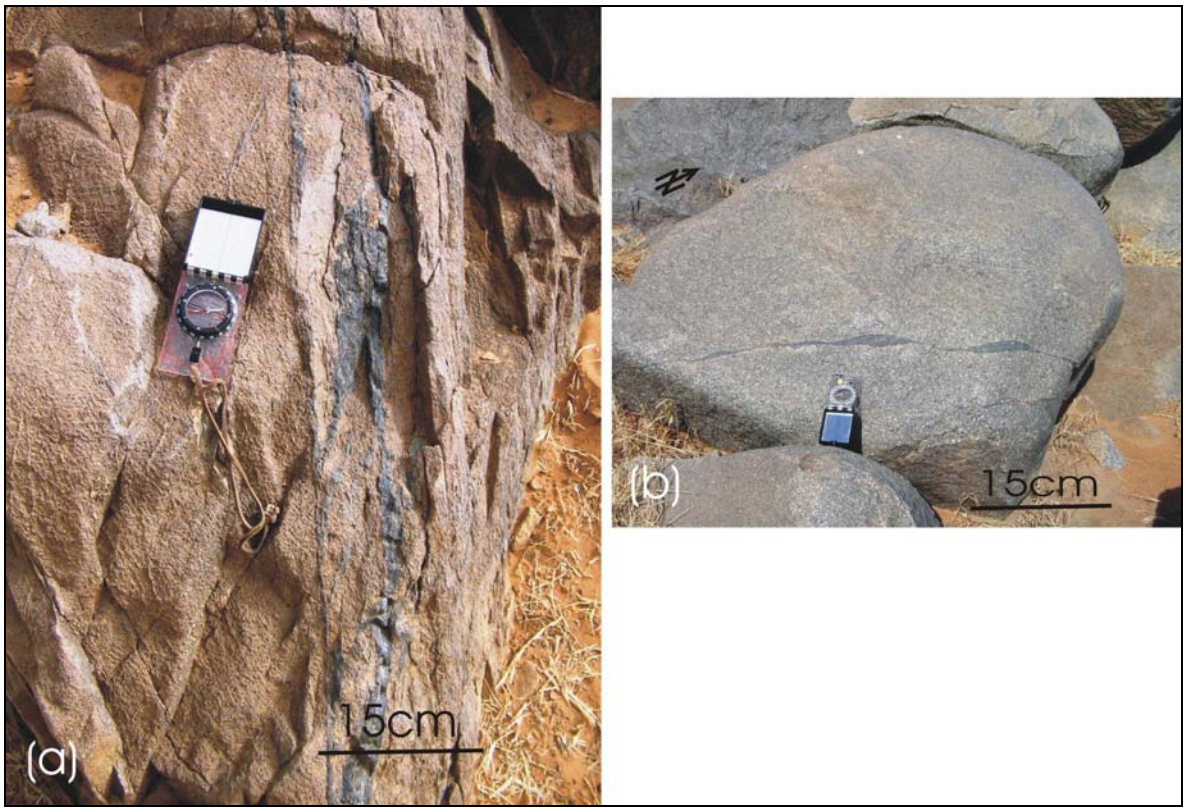

Figure 17. Pseudotachylyte veins crosscutting the (a) adamellite (GPS, N 14 34 57 9 W 00 02 03 6) and (b) granodiorite (GPS, N 14 32 40 6 W 00 00 39 2).

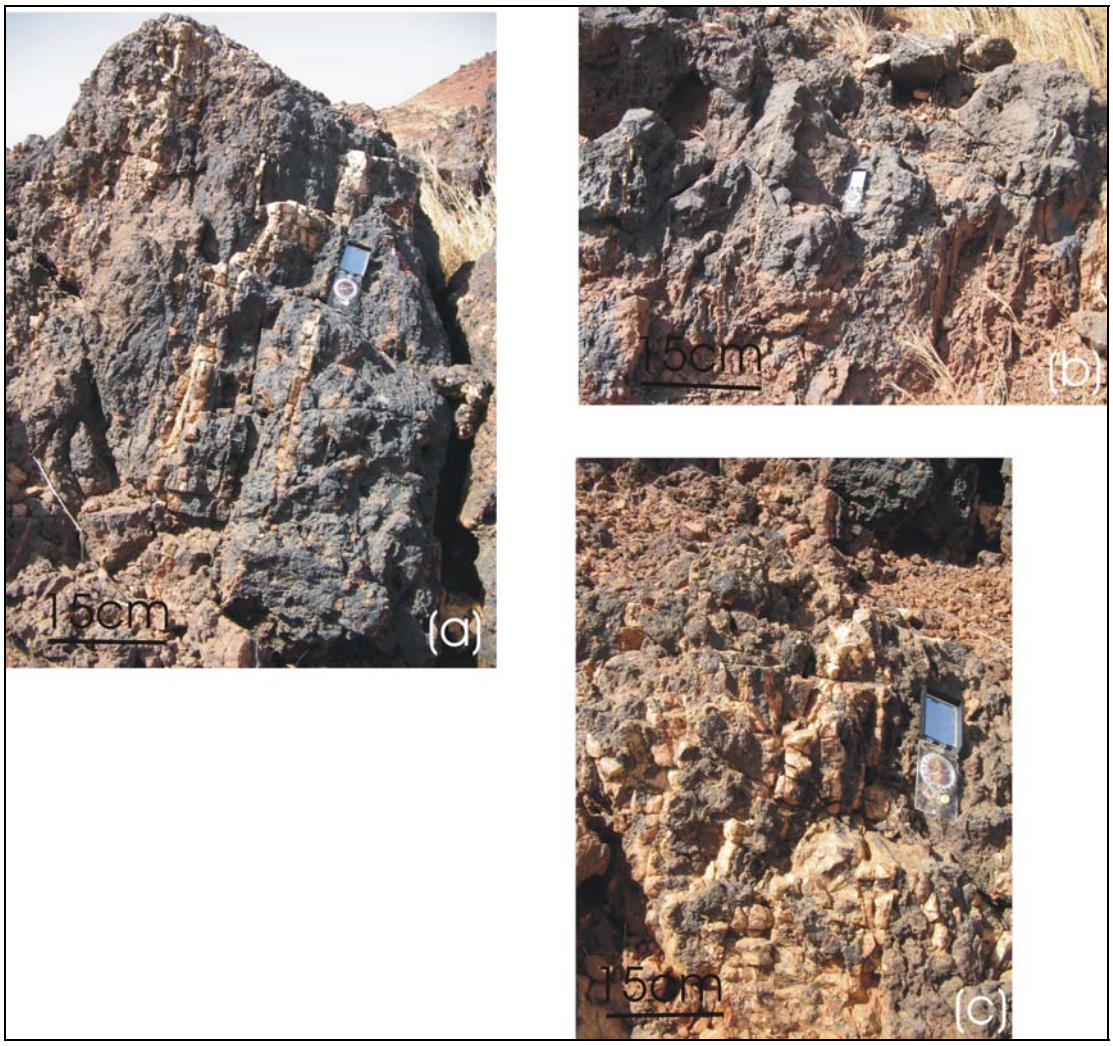

Figure 18. (a, b, c) Quartz iron-rich cataclasite veins in the Markoye fault. The quartz iron-rich cataclasite hosts quartz-carbonate veins. The Orpailleurs happened to be panning gold from the weathered debris of the cataclasite. GPS, N 14 30 53 2 E 00 00 22 6.

Figure 19. Buck-quartz carbonate veins located NE of Tin Taradat Village. The egg box appearance is associated with formation of boudins which plunge steeply. Slickensides are steeply plunging. GPS, N 14 30 47 6 E 00 00 17 7.

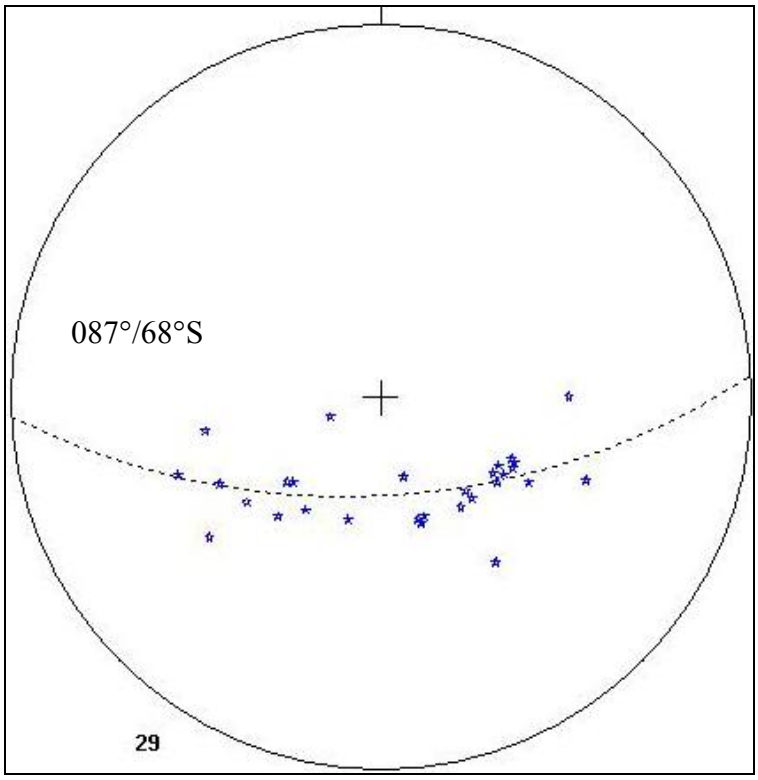

Figure 20. Equal area stereographic projection of L-tectonites. The data lies on the calculated girdle of 087°/ 68°S. This data shows the preferred orientation of the L-tectonites. The mean transport direction is vertical (vertical extension) and slightly to the south.

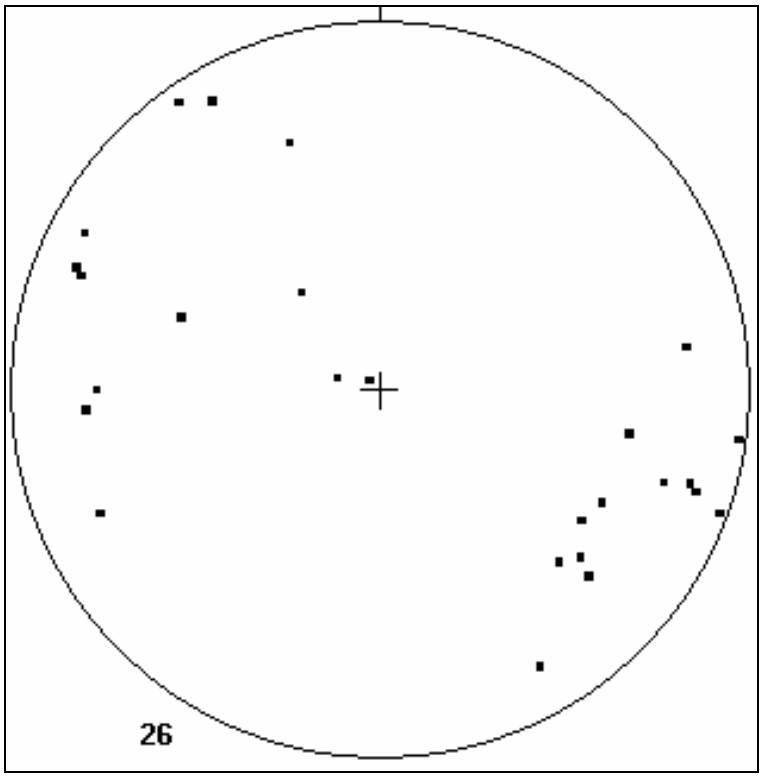

Figure 21. Equal area stereographic projections of poles to schistosity. The calculated mean principal orientation is 025°/86°W. Schistosity represents the reactivation phase in the Markoye fault.

Chapter 6: Discussion

6.1 Meta-sedimentary units and environments of deposition

Although limited by the availability of outcrops due to the Sahara sand dunes, laterite, and alluvial cover, two stratigraphic sequences are recognised in the study area; volcanoclastic and sedimentary. These units are metamorphosed to hornblende-hornfels facies through contact metamorphism, but primary sedimentary structures are preserved as compositional layers (Chapter 4). Primary structures include graded bedding, flaser and cross-bedding, fine laminations, ripple marks, slumps, and scour and fill.

The primary structures indicate a single environment of deposition: shallow marine continental shelf at a delta front setting. The fining up sequence (graded bedding), slumps (gravity flow), mud and sand balls, lithic fragments, ripples, scour and fill, mud-cracks and laminations in meta-volcanoclastic greywacke sequences suggest that the setting was subjected to tidal and or turbidity currents (Eriksson et al., 1998; 2005; Sultan and Björklund, 2006). The upward-fining, laminations, slumps, lithic fragments, and graded beds, with scour and fill bases, are characteristic of turbidity currents that operates at a delta front (Shanmugan, 1997; Sultan and Björklund, 2006), and the ripples are characteristic of tidal currents (Sultan and Björklund, 2006).

The presence of black shale and siltstone at Essakane provides evidence of fine material deposited by suspension settling at the delta front (Eriksson et al., 1998; Sultan and Björklund, 2006). The meta-volcanoclastic greywackes host thin intercalated layers of fuchsite and mud-cracks. Fuchsite layers and mud-cracks can form in lagoonal (continental shelf) environments were temperature and availability of water is the controlling factors (Sultan and Björklund, 2006). The meta-conglomerate contains sub-rounded to rounded clasts indicating a local origin and short transportation distance. The conglomerate units were probably deposited proximal to the source in a deltaic environment (Eriksson et al., 1998). The presence of stromatolites in greywacke

sandstone also suggest shallow marine environment of deposition with high sea salinity (Altermann, 2002; Eriksson et al., 2005).

6.2 Tarkwa Group

The conglomerate units classified as Tarkwa Group consists of greater than 90% rounded vein quartz pebbles, and 10% schist and quartzite pebbles in black sand matrix (Milési et al., 1989, 1991; Bossière et al., 1996). However the meta-conglomerate defined in the study area consists of sub-angular to sub-rounded clasts and boulders of basalt, andesite, granodiorite, granite, volcanoclastic meta-sediments, chert, and lithic fragments in greenish-grey greywacke-lithic matrix. The meta-conglomerate is therefore by no means similar to the meta-conglomerate described for the Tarkwa type section in Ghana. The meta-sedimentary rocks classified as Tarkwa Group by Castaing et al. (2003) are reclassified as Birimian flysch type sediments, as described by Milési et al. (1989).

6.3 Relative chronology of intrusions

The relative chronology of igneous events is based on crosscutting relationships. The volcano-sedimentary and sedimentary rocks of the study area are intruded by adamellite (granite), granodiorite-tonalite, pyroxenite-gabbro, and lastly, dolerite dykes. The adamellite was deformed during D1 and D2. The granodiorite-tonalite intrusions have been classified as a syn-Eburnean in age by Milési et al. (1989), Abouchami and Boher, (1990), Boher et al. (1992), Pons et al. (1995), Oberthür et al. (1998), and Béziat et al. (2000) and contain enclaves of adamellite. The granodiorite-tonalite intrusions are therefore younger than the adamellite.

The granodiorite-tonalite contains xenoliths of pyroxenite-gabbro and it is crosscut by S2 and pseudotachylyte veins. The pyroxenite-gabbro intrusion is also crosscut by S2. The granodiorite-tonalite intrusions are therefore younger than the pyroxenite-gabbro intrusion.

Four emplacement events can therefore be accounted for in the study area, i.e., (1) emplacement of the adamellite (granite), syn- to post-Birimian sedimentation; (2) emplacement of pyroxenite-gabbro; (3) emplacement of granodiorite-tonalite; (4) and the emplacement of dolerite dykes.

6.4 Relative chronology of structural and metamorphic events

Two phases of deformation are recognised related to the Markoye Shear Zone (MSZ) in the area. The first deformation event (D1) is related to the development of NW-trending folds (F1) and this event has been recorded by Ouedraogo and Prost (1986), Feybesse et al. (1990) and Hein et al. (2004. The meta-sedimentary rocks of the Birimian (sandstone and siltstone sequence) are folded about NW-trending fold axes. The palaeo-principle stress orientation during the time is interpreted as SW-directed, and this orientation would have dextrally displaced the MSZ.

The second deformation event (D2) is related to NW-SE crustal shortening (Lompo et al., 1991; Feybesse et al., 2006) and formation of NE-trending folds (F2), and NE-trending cleavage (S2). D2 is related to formation of regional NE-trending C-S foliation, shears, and faults (Ouedraogo and Prost, 1986; Feybesse et al., 1990; Lompo et al., 1991; Hein et al., 2004) and mylonite, pseudotachylyte veins, quartz iron-rich cataclasite veins, buck quartz-carbonate (± tourmaline) veins and quartz-chlorite shears in the study area. D2 is also related to syn-tectonic emplacement of the granodiorite-tonalite plutons in the study area and is consistent with regional interpretation of Boher et al. (1992), Pons et al. (1995), Béziat et al. (2000), Hein et al. (2004) and Naba et al. (2004) of pluton emplacement during the Eburnean Orogeny. D2 is characterised by sinistral (reverse) displacement on the MSZ (Fig. 16).

Displacement during D2 created dilational structures that where filled with silica-rich. It is suggested that this fluids deposited gold-bearing sulphides (Milési et al., 1989).

The early phase of D2 is associated with medium to high grade metamorphic conditions with high strain along the MSZ and formation of the MMZ and pseudotachylyte veins (Fig. 2). Quartz iron-rich cataclasite veins and buck quartz-carbonate (± tourmaline) veins in quartz-chlorite shears crosscut the MMZ and are interpreted to represent low strain rates during progressive deformation on the MSZ. Quartz-chlorite shear zones are gold bearing at Essakane goldfield.

6.5 Relative and Absolute chronologies (Tectonic history)

Although absolute dating can delineate separate stratigraphic sequences and tectonic events based on heavy or light mineral analysis, these minerals are rarely available and the analyses are limited by availability of resources. Due to geological processes that are continuously taking place, including, erosion, deposition and tectonic events, complete stratigraphic sequences are rarely available to define absolute ages, and therefore, it is generally simple to establish the spatial and temporal relationship of the various geological features in the region by establishing the crosscutting relationships. The relative chronology (tectonic history) of the study area is summarised below from the oldest to the youngest.

1. A protolith composed of volcanic-plutonic terrain of granite, granodiorite, basalt, and andesite is interpreted as the source rocks to the Birimian sediments.
2. Erosion and development of a regional unconformity (Milési et al., 1989; Davis et al., 1994; Feybesse and Milési., 1994).
3. Deposition of Birimian sediments including (1) intercalated layers of conglomerate (that have clasts of granite, basalt, andesites, granodiorite, volcanoclastic meta-sedimentary, chert, and lithic fragments), (2) greywackes sandstone, (3) shale, and (4) siltstone units.
4. Intrusion of the pyroxenite-gabbro pluton (YMC) (Béziat et al., 2000; Hein et al., 2004). It contact metamorphosed the wall rock to hornblende-hornfels facies and contains xenoliths of the wall rock. It is crosscut by S2.
5. Intrusion of adamellite (granite).

6. D1. Development of NW-trending asymmetric folds (F1) and thrusts during SW-directed compression.
7. D2. Development of NE-trending foliation (S2), NE-trending folds (F2), and refolding of D1 structures during the NW-SE crustal shortening. This is interpreted as part of the Eburnean Orogeny.
8. Intrusion of syn-orogenic granodiorite-tonalite bodies. The intrusion hosts mafic and sedimentary xenoliths. Contact metamorphism of the wall rock to hornblende-hornfels facies.
9. Development of Mukosi Mylonite Zone (MMZ) and pseudotachylyte veins during sinistral (reverse) displacement (east block down) on the MSZ. The MMZ crosscuts meta-sedimentary rocks and plutons.
10. Reactivation of MSZ. Quartz-chlorite shears which hosts stockwork and brecciated quartz-carbonate (± tourmaline) veins that crosscut the meta-sedimentary rocks. Sulphides are hosted in the fractures and alteration zones of these veins. Gold mineralization has a spatial and temporal relationship with the quartz-chlorite shears. Schistosity crosscuts the YMC and the MMZ.
11. Emplacement of dolerite dykes and contact metamorphism of meta-sedimentary rocks to hornblende-hornfels facies.
12. Development of laterite (Ferricrete) and alluvial profile.

Absolute geochronology has been conducted in some parts of the West African Craton and the dates are presented in Figure 22. Figure 22 plots the age of the Birimian sequences, granitoids, Eburnean Orogeny, gold mineralization and Tarkwa Group sediments. The geochronological data is confusing. The deposition of the Birimian sequences and the Tarkwa sediment, and the emplacement of Eburnean plutons, all give the same approximate absolute ages. This may be the results of imprecision of various dating techniques used, errors on sample collection (xenocrystic zircons in plutonic rocks) or a number of other reasons. However the relative chronology is clear on some parts.

(1) Stratigraphically it is well known from field studies (Milési et al., 1989, 1992; Leube et al., 1990; Davis et al., 1994; Castaing et al., 2003; Tunks et al., 2004) that the Tarkwa Group sediments lie unconformably on the Birimian sequences, and sourcing Birimian sediments (Leube et al., 1990; Milési et al., 1991). In the Figure 22 there is only one data set which agrees with this field observation. All the ages for Tarkwa Group are the same as the Birimian sequences, leading to a conclusion that the Tarkwa Group was deposited at the same time as the Birimian. This is illogical.

(2) Published data and field studies clearly indicate that TTG suite plutons were not emplaced during the deposition of the Birimian sequences. They are syn- to post-Eburnean Orogeny by age (Béziat et al., 2000; Castaing et al., 2003; Hein et al., 2004). However most of the published ages in Figure 22 imply syn-depositional emplacement.

(3) In Figure 22 the ages for granite suite rocks are younger than, or, synchronous to, the emplacement of tonalite suite rocks. At Essakane goldfield granite xenoliths are hosted in tonalite, which means that the granite suite is older than the tonalite suite.

Consequently the data set shows inconsistencies and this needs further investigation.

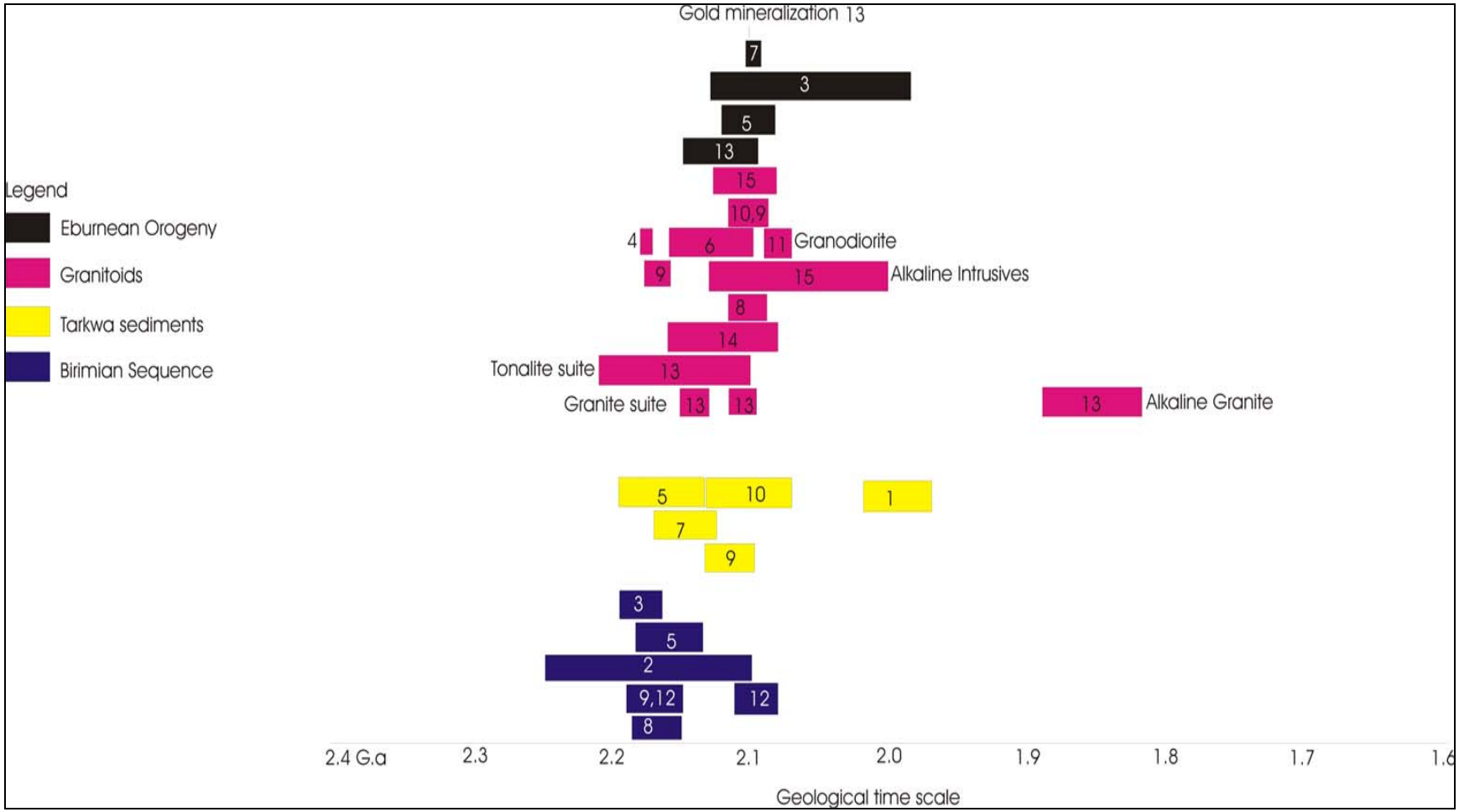

Figure 22. Published absolute geochronology for rocks of the West African Craton after, 1, 4, 8, Hirdes et al., 1987 (Rb/Sr), 1992, 1996, 2. Milési et al., 1989 (Rb/Sr), 3. Leube et al., 1990, 5.Davis et al., 1994 (U-Pb), 6. Pons et al., 1995, 7. Bossière et al., 1996 (Pb-evaporation), 9, 12.Hirdes and Davis, 1998, 2002 (U-Pb), 10.Oberthür et al., 1998 (U-Pb), 11. Egal et al., 2002 (Pb-evaporation), 13. Castaing et al., 2003(Pb-Pb, K-Ar), 14.Dioh et al., 2006, 15. Feybesse et al., 2006 (Pb-evaporation, Sm-Nd, K-Ar, Ar^{39}/Ar^{40}).

Chapter 7: Conclusion

The Markoye fault is a broad zone of faulting, shearing, mylonite zone, pseudotachylyte veins, L-tectonites, quartz iron-rich cataclasite veins and quartz-carbonate (± tourmaline) veins and is renamed as the Markoye Shear Zone (MSZ).

The lithologies of Essakane goldfield consist of metamorphosed Birimian volcano-sedimentary and sedimentary sequences that were deposited in a shallow marine continental shelf at a delta front setting. These sequences have been intruded by plutonic rocks that include granodiorite-tonalite, pyroxenite-gabbro, granite (adamellite) plutons and dolerite dykes. The plutons and dyke systems have contact metamorphosed the rocks of the region to hornblende-hornfels facies, but primary sedimentary structures are preserved as compositional layers. All the lithologies in the area have been subjected to several phases of local-regional deformation, with development of mylonite, schistosity, and L-tectonite.

Two phases of deformation are recognised related to the Markoye Shear Zone (MSZ) in the area. D1 pre-dates the Eburnean deformation. This deformation is characterised by asymmetric NW-trending folds (F1) axes planes with the principal transport to the SW.

The D2 is characterised by the development of the MMZ, pseudotachylyte veins, quartz iron-rich cataclasite veins, and buck-quartz carbonate veins, with sinistral reverse displacement, east block down along the MSZ, and the refolding of F1 to F2 (NE-trending folds axes planes) and development of NE-trending S2 and is correlated with the Eburnean Orogeny at 2150 to 2095 Ma. The reactivation phase of D2 is characterised by greenschist metamorphic facies with sinistral displacement, west block down along the MSZ, stockwork, and breccia veins that are sulphides bearing.

The above data indicates that the MSZ have a long tectonic history. This first order crustal scale structure has been active pre-, syn-, to post- Eburnean Orogeny, and it is not a Pan African in age. The gold mineralization in the Essakane goldfield is related to the late quartz-chlorite schist of D2.

References:

Abouchami, W., Boher, M., 1990. A major 2.1 Ga event of mafic magmatism in West Africa: and early stage of crustal accretion. Journal of Geophysical Research 95 (B11), 17605-17629.

Altermann, W., 2002. The evolution of life and its impact on sedimentation. In: Altermann, W., Corcoran, P.L. (Eds.), Precambrian sedimentary environments: A modern approach to ancient depositional systems. Special Publication, The International Association of Sedimentologists 33, 15-32.

Béziat, D., Bourges, F., Debat, P., Lompo, M., Martin, F., Tollon, F., 2000. A Paleoproterozoic ultramafic-mafic assemblage and associated volcanic rocks of the Boromo greenstone belt: fractionates originating from island-arc volcanic activity in the West African craton. Precambrian Research 101, 25-47.

Boher, M., Abouchami, W., Michard, A., Albarede, F., Arndt, N.T., 1992. Crustal growth in West Africa at 2.1 Ga. Journal of Geophysical Research 97 (B1), 345-369.

Bossière, G., Bonkoungou, I., Peucat, J.J., Pupin, J.P., 1996. Origin and age of Palaeoproterozoic conglomerates and sandstones of the Tarkwaian Group in Burkina Faso, West Africa. Precambrian Research 80, 153-172.

Brown, E.T., Bourlès, D.L., Colin, F., Safno, Z., Raisbeck, G.M., Yiou, F., 1994. The development of iron crust lateritic systems in Burkina Faso, West Africa examined with in-situ-produced cosmogenic nuclides. Earth and Planetary Science Letters 124, 19-33.

Castaing, C., Billa, M., Milési, J.P., Thiéblemont, D., Le Mentour, J., Egal, E., Donzeau, M. (BRGM) (coordonnateurs) et Guerrot, C., Cocherie, A., Chevremont, P., Tegyey, M., Itard, Y. (BRGM), Zida, B., Ouedraogo, I., Kote, S., Kabore, B.E., Ouedraogo, C. (BUMIGEB), Ki, J.C., Zunino (ANTEA), 2003. Notice explicative de la Carte géologique et miniére du Burkina Faso à 1/1 000 000.

Castaing, C., Le Mentour, J., Billa, M., (coordonnateurs) et Donzeau, M., Chevremont, P., Egal, E. (BRGM), Zida, B., Ouedraogo, I., Kote, S., Kabore, B.E., Ouedraogo, C. (BUMIGEB), Thiéblemont, D., Guerrot, C., Cocherie, A., Tegyey, M., Milési, J.P., Itard, Y., (BRGM), 2003. Carte géologique et miniére du Burkina Faso à 1/1 000 000.

Davis, D.W., Hirdes, W., Schaltegger, U., Nunoo, E.A., 1994. U-Pb age constraints on deposition and provenance of Birimian and gold-bearing Tarkwaian sediments in Ghana, West Africa. Precambrian Research 67, 89-107.

Davis, G.H., Reynolds, S.J., 1996. Structural geology of rocks and regions. John Wiley and Sons, Inc, Canada, p.775.

Delisle, P.C., 2003. Structural analysis of the Essakane deposit Burkina Faso, West Africa. Company report (unpublished), Orezone Resources Inc. Ottawa, Canada, 3p.

Dequincey, O., Chabaux, F., Leprun, J.C., Panquet, H., Clauer, N., Larque, P., 2006. Lanthanide and trace elements mobilization in a lateritic toposequence: inferences from the Kaya laterite in Burkina Faso. European Journal of Soil Science 57, 816-830.

Dioh, E., Béziat, D., Debat, P., Grégoire, M., Ngom, P.M., 2006. Diversity of the Palaeoproterozoic granitoids of the Kédougou Inlier (eastern Sénégal): petrographical and geochemical constraints. Journal of African Earth Sciences 44, 351-371.

Egal, E., Thiéblemont, D., Lahondère, D., Guerrot, C., Costea, C.A., Iliescu, D., Delor, C., Goujou, J.C., Lafon, J.M., Tegyey, M., Diaby, S., Kolié, P., 2002. Late Eburnean granitization and tectonics along the western and northwestern margin of the Archean Kénéma-Man domain (Guinea, West African Craton). Precambrian Research 117, 57-84.

Eriksson, P.G., Condie, K.C., Tirsgaard, H., Mueller, W.U., Altermann, W., Miall, A.D., Aspler, L.B., Catuneanu, O., Chiarenzelli, J.R., 1998. Precambrian clastic sedimentation systems. Sedimentary Geology 120, 5-53.

Eriksson, P.G., Catuneanu, O., Sarkar, S., Tirsgaard, H., 2005. Patterns of sedimentation in the Precambrian. Sedimentary Geology 176, 17-42.

Feybesse, J.L., Billa, M., Guerrot, C., Duguey, E., Lescuyer, J.L., Milési, J.P., Bouchot, V., 2006. The Palaeoproterozoic Ghanaian province: Geodynamic model and ore controls, including regional stress modelling. Precambrian Research 149, 149-196.

Feybesse, J.L., Milési, J.P., 1994. The Archaean/Proterozoic contact zone in West Africa: a mountain belt of decollement thrusting and folding on a continental margin related to 2.1 Ga convergence of Archaean cratons? Precambrian Research 69, 199-227.

Feybesse, J.L., Milési, J.P., Ouedraogo, M.F., Prost, A., 1990. La "ceinture" protérozoïque inférieur de Boromo-Goren (Burkina Faso): un exemple d'interférence entre deux phases transcurrentes éburnéennes. Comptes Rendus de L'Académie des Sciences 310, II, 1353-1360.

Foster, R.P., Piper, D.P., 1993. Archaean lode gold deposits in Africa: crustal setting, metallogenesis and cratonization. Ore Geology Reviews 8, 303-347.

Hastings, D., 1982. On the tectonics and metallogenesis of West Africa: A model incorporating new geophysical data. Geoexploration 20, 295-327.

Hein, K.A.A., Morel, V., Kagoné, O., Kiemde, F., Mayes, K., 2004. Birimian lithological succession and structural evolution in the Goren segment of the Boromo-Goren Greenstone belt, Burkina Faso. Journal of African Earth Sciences 39, 1-23.

Hein, K.A.A, Tshibubudze, A., 2007. Relative chronology of tectonic events in the region east of Gorom Gorom, Burkina Faso. Unpublished report Report 2 to Ore Zone Resources, 15p.

Hirdes, W., Davis, D.W., 1998. First U-Pb zircon age of extrusive volcanism in the Birimian Supergroup of Ghana/West Africa. Journal of African Earth Sciences 27, 291-294.

Hirdes, W., Davis, D.W., 2002. U-Pd geochronology of Palaeoproterozoic rocks in the southern part of the Kedougou-Kéniéba Inlier, Senegal, West Africa: Evidence for diachronous accretionary development of the Eburnean province. Precambrian Research 118, 83-99.

Hirdes, W., Davis, D.W., Eisenlohr, B.N., 1992. Reassessment of Proterozoic granitoid ages in Ghana on basis of U/Pb zircon and monazite dating. Precambrian Research 56, 89-96.

Hirdes, W., Davis, D.W., Lüdtke, G., Konan, G., 1996. Two generations of Birimian (Paleoproterozoic) volcanic belts in north-eastern Côte d'Ivoire (West Africa): consequences for the 'Birimian Controversy'. Precambrian Research 80, 173-191.

Hirdes, W., Saager, R., Leube, A., 1987. The Tarkwaian group of Ghana: new aspects to its tectonic setting, structural evolution, gold mineralization and provenance area.

Holcombe, R., 2006. Stereographic projections and rose diagrams plots. Holcombe Caughlin_Associates, Australia. [http://www.holcombe.net.au/software/].

Hottin, G., Ouedraogo, O.F., 1992. Carte Géologique du Burkina Faso (2nd edition). Bureau de Recherches Géologique et Miniéres, Burkina Faso.

Leube, A., Hirdes, W., Mauer, R., Kesse, G.O., 1990. The early Proterozoic Birimian Supergroup of Ghana and some aspects of its associated gold mineralization. Precambrian Research 46, 139-165.

Liégeois, J.L., Latouche, L., Boughara, M., Navez, J., Guiraud, M., 2003. The LATEA metacraton (Central Hoggar, Tuareg shield, Algeria): behaviour of an old passive margin during the Pan-African orogeny. Journal of African Earth Sciences 37, 161-190.

Lompo, M., 2001. Le Paléoprotérozoïque (Birimien) du Burkina Faso Afrique de l′Ouest Évolution crustale et concentrations aurifères. UFR/ SVT Département de Géologie, Équipes de Pétrophysique et Tectonique, Universite de Ouagadougou, 135p.

Lompo, M., Caby, R., Robineau, B., 1991. Évolution structurale du Birimien au Burkina Faso: exemple dela ceinture de Boromo-Goren dans le secteur de Kwademen (Afrique de l'Ouest). Comptes Rendus de l'Académie des Sciences de Paris, Série II 313, 954-950.

Milési, J.P., Feybesse, J.L., Ledru, P., Dommanget, A., Ouedraogo, M.F., Marcoux, E., Prost, A., Vinchon, Ch., Sylvain, J.P., Johan, V., Tegyey, M., Calvez, J.Y., Lagny, P. 1989. West African gold deposits, in their lower Proterozoic lithostructural setting. Chronique de la Recherché Minière 497, 3-98.

Milési, J.P., Ledru, P., Ankrah, P., Johan, V., Marcoux, E., Vinchon, Ch., 1991. The metallogenic relationship between Birimian and Tarkwaian gold deposits in Ghana. Mineralium Deposita 26, 228-238.

Milési, J.P., Ledru, P., Feybesse, J.L., Dommanget, A., Marcoux, E., 1992. Early Proterozoic ore deposits and tectonics of the Birimian orogenic belt, West Africa. Precambrian Research 58, 305-344.

Naba, S., Lompo, M., Debat, P., Bouchez, J.L., Béziat, D., 2004. Structure and emplacement model for late-orogenic Palaeoproterozoic granitoids: the Tenkodogo-Yamba elongate pluton (Eastern Burkina Faso). Journal of African Earth Sciences 38, 41-57.

Navas, A.S., Reddy, B.J., Nieto, F., 2004. Spectroscopic study of chromium, iron, OH, fluid and mineral inclusions in uvarovite and fuchsite. Spectrochimica Acta Part A 60, 2261-2268.

Oberthür, T., Vetter, U., Davis, D.W., Amanor, J.A., 1998. Age constraints on gold mineralization and Paleoproterozoic crustal evolution in the Ashanti belt of southern Ghana. Precambrian Research 89, 129-143.

Ouedraogo, M.F., Prost, A.E., 1986. Mise en evidence des relations entre schistosites et plissements dans la ceinture volcanique birrimienne de Yako-Batié (Burkina Faso). Comptes Rendus de l'Académie des Sciences de Paris, Série II 303, 1713-1718.

Pawlig, S., Gueye, M., Klischies, R., Schwarz, S., Wemmer, K., Siegesmund, S., 2006. Geochemical and Sr-Nd isotopic data on the Birimian of the Kedougou-Kenieba Inlier (Eastern Senegal): Implications on the Palaeoproterozoic evolution of the West African Craton. South African Journal of Geology 109, 411-427.

Pons, J., Barley, P., Dupuis, D., Léger, J.M., 1995. Mechanisms of pluton emplacement and structural evolution of a 2.1 G.a juvenile continental crust: the Birimian of south western Niger. Precambrian Research 70, 281-301.

Rogers, J. and Dong, F., 2000. Technical Report-Essakane Prospect, Burkina Faso, Company report (unpublished). ABOSSO Goldfields Limited, Accra, Ghana, 14p.

Shanmugan, G., 1997. The Bouma sequences and turbidite mind set. Earth-Science Reviews 42, 201-229.

Sultan, L., Björklund, P.P., 2006. Depositional environments at a Palaeoproterozoic continental margin, Västervik basin, SE Sweden. Precambrian Research 145, 243-271.

Thiéblemont, D., Delor, C., Cocherie, A., Lafon, J.M., Goujou, J.C., Baldé, A., Bah, M., Sané, H., Fanning, C.M., 2001. A 3.5 Ga granite-gneiss basement in Guinea: further evidence for early Archaean accretion within the West African Craton. Precambrian Research 108, 179-194.

Thiéblemont, D., Goujou, J.C., Egal, E., Cocherie, A., Delor, C., Lafon, J.M., Fanning, C.M., 2004. Archaean evolution of the Leo Rise and its Eburnean reworking. Journal of African Earth Sciences 39, 97-104.

Tunks, A.J., Selley, D., Rogers, J.R., Brabham, G., 2004. Vein mineralization at the Damang gold mine, Ghana: controls on mineralization. Journal of Structural Geology 26, 1257-1273.

Appendix A. Table of Field Data.										
STN	**NORTHINGS**	**EASTINGS**	**WESTINGS**	**HOST ROCK TYPE**	**STR**	**DIP**	**DIP DIR**	**STRU**	**FACING**	**SAMPLE NOS**
001	14 97 02 1	07 92 92 6		Subcrop, siltstone and quartz vein						
002	14 97 72 7	07 92 66 3		Greywacke-siltsone sequence	010	86	E	BEDDING	E	
002	14 97 72 7	07 92 66 3		Greywacke-siltsone sequence	028	60	W	CLEAVAGE		
002	14 97 72 7	07 92 66 3		Greywacke-siltsone sequence	042	89	E	QUARTZ VEIN		
003	14 97 94 4	07 92 50 4		Greywacke-siltsone sequence	034	74	W	BEDDING	E	
003	14 97 94 4	07 92 50 4		Greywacke-siltsone sequence	030	82	E	CLEAVAGE		
003	14 97 94 4	07 92 50 4		Greywacke-siltsone sequence	064	78	W	CLEAVAGE		
003	14 97 94 4	07 92 50 4		Greywacke-siltsone sequence				QUARTZ VEIN		
004	14 98 00 8	07 92 41 1		Schistosed sandstone	042	87	W	CLEAVAGE		004
004	14 98 00 8	07 92 41 1		Schistosed sandstone	051	62	W	CLEAVAGE		
005	14 38 58 8	00 03 47 5		Volcanoclastic greywacke	354	74	E	BEDDING		005
006	14 38 54 3	00 03 47 9		Massive volcanoclastic greywacke	352	64	E	BEDDING	E	
006	14 38 50 2	00 03 42 6		Massive volcanoclastic greywacke	354	54	E	BEDDING	E	
007	14 38 30 7	00 03 36 2		Massive volcanoclastic greywacke	009	39	E	BEDDING		
008	14 38 23 1	00 03 32 6		Massive volcanoclastic greywacke	010	56	E	BEDDING		008
008	14 38 23 1	00 03 32		Massive volcanoclastic greywacke	014			DYKE		

		6								
009	14 38 03 3	00 03 32 8		Volcanoclastic greywacke	023	53	E		E	
009	14 38 03 3	00 03 32 8		Volcanoclastic greywacke	296			DYKE		
010	14 38 00 0	00 03 31 6		Volcanoclastic greywacke	010	60	E		E	
011	14 37 54 4	00 03 27 3		Massive volcanoclastic greywacke	351	48	E		E	011
012	14 36 07 0	00 01 34 8		Felsic Granite						012
013										
014	14 25 16 6	00 02 41 0		Gabbro dyke	166			DYKE		014
015	14 25 17 5	00 02 37 8		Hornfels	312	46	E	BEDDING	E	
016A				Buck-quartz carbonate vein	023			TREND		
016A	14 28 09 1		00 00 08 0	Buck-quartz carbonate vein						
016A	14 28 11 6		00 00 06 1	Buck-quartz carbonate vein						
016A	14 28 10 8		00 00 06 4	Buck-quartz carbonate vein						
016A	14 28 07 9		00 00 08 0	Buck-quartz carbonate vein						
016A	14 28 07 1		00 00 08 0	Buck-quartz carbonate vein						
016B	14 27 57 5		00 00 12 1	Buck-quartz carbonate vein	042	65	W	CLEAVAGE		
016B	14 27 57 5		00 00 12 1	Buck-quartz carbonate vein	017	77	W	CLEAVAGE		
016B	14 27 57 5		00 00 12 1	Buck-quartz carbonate vein		45	200	LINEATION		
016B	14 27 56 4		00 00 12 5	Buck-quartz carbonate vein						
016B	14 27 55 7		00 00 12	Buck-quartz carbonate vein						

			2							
016B	14 27 54 7		00 00 11 9	Buck-quartz carbonate vein	040	60	W	CLEAVAGE		
016B	14 27 53 5		00 00 12 2	Buck-quartz carbonate vein	000	66	E	CLEAVAGE		
016B	14 27 53 5		00 00 12 2	Buck-quartz carbonate vein	021	76	E	CLEAVAGE		
016B	14 27 52 5		00 00 12 2	Buck-quartz carbonate vein						
016B	14 27 55 9		00 00 14 0	Buck-quartz carbonate vein						
016B	14 27 53 1		00 00 14 7	Buck-quartz carbonate vein						
016C	14 27 48 0		00 00 14 0	Buck-quartz carbonate vein						
016C	14 27 46 8		00 00 14 3	Buck-quartz carbonate vein						
016C	14 27 46 5		00 00 14 2	Buck-quartz carbonate vein	309	37	N	FAULT		
016C	14 27 46 5		00 00 14 2	Buck-quartz carbonate vein		9	116	LINEATION		
016C	14 27 45 3		00 00 14 3	Buck-quartz carbonate vein						
016C	14 27 44 2		00 00 14 7	Buck-quartz carbonate vein	016	10	E	CLEAVAGE		
016C	14 27 44 5		00 00 17 4	Buck-quartz carbonate vein	022	54	E			
017	14 27 44 5		00 00 17 4	Chlorite mica schist	356	69	E	CLEAVAGE		017
017	14 27 44 5		00 00 17 4	Chlorite mica schist	013	90		CLEAVAGE		
017	14 27 44 5		00 00 17 4	Chlorite mica schist	020	88	W	CLEAVAGE		
017	14 27 44 5		00 00 17 4	Chlorite mica schist	008	88	W			
018				Buck-quartz carbonate vein	016			TREND		

018A	14 29 20 4	00 00 05 9		Buck-quartz carbonate vein		52	232	LINEATION		018 A
018A	14 29 20 4	00 00 05 9		Buck-quartz carbonate vein		50	259	LINEATION		
018A	14 29 20 4	00 00 05 9		Buck-quartz carbonate vein		49	242	LINEATION		
018A	14 29 20 4	00 00 05 9		Buck-quartz carbonate vein		40	231	LINEATION		
018A	14 29 20 4	00 00 05 9		Buck-quartz carbonate vein		41	249	LINEATION		
018A	14 29 15 5	00 00 01 9		Buck-quartz carbonate vein						
018A	14 29 11 5	00 00 04 4		Buck-quartz carbonate vein						
018A	14 29 10 8	00 00 03 9		Buck-quartz carbonate vein						
018A	14 29 09 3	00 00 03 2		Buck-quartz carbonate vein						
018A	14 29 07 9	00 00 02 0		Buck-quartz carbonate vein						
018A	14 29 06 8	00 00 01 4		Buck-quartz carbonate vein						
018A	14 29 02 1	00 00 01 1		Buck-quartz carbonate vein						
018A	14 28 59 7		00 00 00 0	Buck-quartz carbonate vein						
018B	14 28 59 4		00 00 00 0	Buck-quartz carbonate vein						
018B	14 28 58 4		00 00 00 4	Buck-quartz carbonate vein						
018B	14 28 57 4		00 00 00 7	Buck-quartz carbonate vein						
018C	14 28 54 3		00 00 01 4	Buck-quartz carbonate vein						
018D	14 28 34 9		00 00 04 5	Buck-quartz carbonate vein						

019	14 29 21 2	00 00 10 3		Pyroxenite						019
020	14 29 34 3	00 00 10 3		Pyroxenite						
021	14 29 33 3	00 00 16 7		Gabbro						
022	14 29 33 6	00 00 19 0		Gabbro						022
023	14 29 43 1	00 00 22 4		Gabbro dyke						
024	14 29 43 1	00 00 14 1		Gabbro dyke	026			TREND		
025	14 30 12 5	00 00 16 2		Pyroxenite	060	76	N	CLEAVAGE		
026	14 30 13 1	00 00 18 3		Pyroxenite	022	78	E	CLEAVAGE		
026	14 30 13 1	00 00 18 3		Pyroxenite	060	80	E	CLEAVAGE		
027	14 30 14 5	00 00 24 2		Gabbro	018	70	W			027
028	14 30 16 8	00 00 28 1		Gabbro						028
029	14 30 16 6	00 00 31 1		Gabbro						
030	14 30 32 2	00 00 35 0		Contact aureole hornfels						
031	14 30 43 9	00 00 39 3		Hornfels	080	62	S			
032	14 30 43 9	00 00 38 8		Contact aureole hornfels						
033	14 30 59 8	00 00 38 9		Pyroxenite						
034	14 30 59 8	00 00 27 2		Laterite	060			TREND		
035	14 30 53 2	00 00 22 6		Cataclasite	060			TREND		035

036	14 30 51 6	00 00 22 0		Chlorite quartz mica schist	000		E	TREND		
037	14 30 27 7	00 00 22 7		Pyroxenite						
038	14 30 17 1	00 00 16 2		Pyroxenite						
039	14 30 36 8	00 00 27 5		Pyroxenite						
040	14 30 43 0	00 00 27 1		Laterite						
041	14 30 52 1	00 00 20 1		Meta-sediments		52	120	LINEATION		
041	14 30 52 1	00 00 20 1		Meta-sediments		57	116	LINEATION		
041	14 30 52 1	00 00 20 1		Meta-sediments		58	115	LINEATION		
041	14 30 52 1	00 00 20 1		Meta-sediments		48	090	LINEATION		
041	14 30 52 1	00 00 20 1		Meta-sediments		60	124	LINEATION		
041	14 30 52 1	00 00 20 1		Meta-sediments		62	138	LINEATION		
041	14 30 52 1	00 00 20 1		Meta-sediments		60	138	LINEATION		
041	14 30 52 1	00 00 20 1		Meta-sediments		40	112	LINEATION		
041	14 30 52 1	00 00 20 1		Meta-sediments		58	126	LINEATION		
041	14 30 52 1	00 00 20 1		Meta-sediments		60	120	LINEATION		
041	14 30 52 1	00 00 20 1		Meta-sediments		58	122	LINEATION		
041	14 30 52 1	00 00 20 1		Meta-sediments		57	118	LINEATION		
041	14 30 52 1	00 00 20 1		Meta-sediments	336	72	E	CLEAVAGE		

041	14 30 52 1	00 00 201		Meta-sediments		60	144	LINEATION		
042A	14 30 38 7	00 00 195		Buck-quartz carbonate vein		62	195	LINEATION		
042A	14 30 38 7	00 00 195		Buck-quartz carbonate vein		78	249	LINEATION		
042A	14 30 40 1	00 00 190		Buck-quartz carbonate vein						
042B	14 30 418	00 00 181		Buck-quartz carbonate vein		61	162	LINEATION		
042B	14 30 43 1	00 00 182		Buck-quartz carbonate vein						
042C	14 30 43 4	00 00 178		Buck-quartz carbonate vein						
042D	14 30 44 8	00 00 168		Buck-quartz carbonate vein						
042D	14 30 45 7	00 00 167		Buck-quartz carbonate vein						
042E	14 30 47 4	00 00 168		Buck-quartz carbonate vein						
042E	14 30 47 9	00 00 168		Buck-quartz carbonate vein						
042F	14 30 47 8	00 00 164		Buck-quartz carbonate vein						
042F	14 30 47 6	00 00 177		Buck-quartz carbonate vein		62	160	LINEATION		
042F	14 30 47 6	00 00 177		Buck-quartz carbonate vein		62	163	LINEATION		
042F	14 30 47 6	00 00 177		Buck-quartz carbonate vein		72	164	LINEATION		
042F	14 30 48 4	00 00 173		Buck-quartz carbonate vein						
042F	14 30 48 9	00 00 168		Buck-quartz carbonate vein		45	145	LINEATION		
042G	14 30 49 9	00 00 184		Buck-quartz carbonate vein						

042G	14 30 50 7	00 00 17 8		Buck-quartz carbonate vein						
043	14 31 13 7	00 00 29 3		Gabbro	010	90		CLEAVAGE		
043	14 31 13 7	00 00 29 3		Gabbro	033	55	W	CLEAVAGE		
043	14 31 13 7	00 00 29 3		Gabbro	013	90		CLEAVAGE		
043	14 31 13 7	00 00 29 3		Gabbro	044	57	W	CLEAVAGE		
044	14 31 15 5	00 00 25 3		Laterite	035			TREND		
045	14 31 06 8	00 00 14 2		Laterite						
046	14 31 03 4	00 00 14 0		Laterite						
047	14 30 55 9	00 00 14 0		Laterite						
048	14 30 52 4	00 00 16 1		Laterite						
049	14 29 19 6	00 00 10 1		Gabbro						
050	14 29 19 6	00 00 10 1		Meta-lithogreywacke						
051	14 29 19 6	00 00 10 1		Hornblende Hornfels						051
052	14 29 19 6	00 00 10 1		Spotted Hornfels						
053	14 30 54 3	00 00 09 1		Hornfels	000	53	W			
054	14 31 21 1	00 00 13 1		Meta-gritvolcanoclastic greywacke	337	47	E			
055	14 31 10 9	00 00 52 2		Volcanoclastic greywacke						
056	14 31 39 6	00 01 07 0		Gabbro						

057	14 31 48 0	00 01 11 0		Hornfels sandstone breccia						
058	14 32 10 2	00 00 07 2		Gabbro-Pyroxenite	054	90		CLEAVAGE		
058	14 32 10 2	00 00 07 2		Gabbro-Pyroxenite	047	90		CLEAVAGE		
058	14 32 10 2	00 00 07 2		Gabbro-Pyroxenite	055	85	E	CLEAVAGE		
059	14 32 40 6		00 00 39 2	Granodiorite	352	73	W	CLEAVAGE		
059	14 32 40 6		00 00 39 2	Granodiorite	018	79	W	CLEAVAGE		
059	14 32 40 6		00 00 39 2	Granodiorite	037	77	E	FAULT		
059	14 32 40 6		00 00 39 2	Granodiorite		35	190	LINEATION		
059	14 32 40 6		00 00 39 2	Granodiorite	334	82	W	ELONGATION		
059	14 32 40 6		00 00 39 2	Granodiorite	324	86	W	ELONGATION		
059	14 32 40 6		00 00 39 2	Granodiorite	022	82	E	FAULT		
059	14 32 40 6		00 00 39 2	Granodiorite	010	84	E	FAULT		
059	14 32 40 6		00 00 39 2	Granodiorite		50	182	LINEATION		
059	14 32 40 6		00 00 39 2	Granodiorite	349	72	E	FAULT		
059	14 32 40 6		00 00 39 2	Granodiorite	344	82	E	ELONGATION		
059	14 32 40 6		00 00 39 2	Granodiorite	339	80	W	ELONGATION		
059	14 32 40 6		00 00 39 2	Granodiorite	343	86	E	ELONGATION		
060	14 32 47 1		00 01 18 4	Gabbro-norite						

061	14 34 57 9		00 02 03 6	Granodiorite	028	87	E	CLEAVAGE		061
061	14 34 57 9		00 02 03 6	Granodiorite	036	72	E	CLEAVAGE		
061	14 34 57 9		00 02 03 6	Granodiorite		56	198	LINEATION		
061	14 34 57 9		00 02 03 6	Granodiorite	032	90		CLEAVAGE		
061	14 34 57 9		00 02 03 6	Granodiorite	028	72	E	CLEAVAGE		
061	14 34 57 9		00 02 03 6	Granodiorite		28	209	LINEATION		
061	14 34 57 9		00 02 03 6	Granodiorite	082	82	E	CLEAVAGE		
061	14 34 57 9		00 02 03 6	Granodiorite		58	197	LINEATION		
061	14 34 57 9		00 02 03 6	Granodiorite	084	81	N	FAULT		
061	14 34 57 9		00 02 03 6	Granodiorite	048	48	W	FAULT		
061	14 34 57 9		00 02 03 6	Granodiorite	062	83	N	FAULT		
061	14 34 57 9		00 02 03 6	Granodiorite	063	90		FAULT		
061	14 34 57 9		00 02 03 6	Granodiorite	043		E	FAULT		
061	14 34 57 9		00 02 03 6	Granodiorite	046	88	E	FAULT		
061	14 34 57 9		00 02 03 6	Granodiorite	058	88	W	FAULT		
061	14 34 57 9		00 02 03 6	Granodiorite	092	80	S	FAULT		
061	14 34 57 9		00 02 03 6	Granodiorite	044	80	N	FAULT		
061	14 34 57 9		00 02 03 6	Granodiorite	090	81	N	FAULT		

062	14 36 37 8	00 00 12 1		Mylonite-ultramylonite zone	004	86	E	CLEAVAGE		
062	14 36 37 8	00 00 12 1		Mylonite-ultramylonite zone	014	80	E	CLEAVAGE		
063	14 36 39 4	00 00 10 4		Mylonite-ultramylonite zone	063	70	W	CLEAVAGE		
063	14 36 39 4	00 00 10 4		Mylonite-ultramylonite zone	036	78	W	CLEAVAGE		
063	14 36 39 4	00 00 10 4		Mylonite-ultramylonite zone	068	80	W	CLEAVAGE		
063	14 36 39 4	00 00 10 4		Mylonite-ultramylonite zone	034	86	E	CLEAVAGE		
063	14 36 39 4	00 00 10 4		Mylonite-ultramylonite zone	079	71	W	CLEAVAGE		
063	14 36 39 4	00 00 10 4		Mylonite-ultramylonite zone	030	80	E	CLEAVAGE		
064	14 36 43 3	00 00 07 6		Mylonite	034	71	W	CLEAVAGE		064
064	14 36 43 3	00 00 07 6		Mylonite	040	56	W	CLEAVAGE		
064	14 36 43 3	00 00 07 6		Mylonite		53	027	LINEATION		
065	14 36 43 5	00 00 03 0		Mylonitised granitoid	036	82	W	CLEAVAGE		
065	14 36 43 5	00 00 03 0		Mylonitised granitoid		12	216	LINEATION		
066	14 36 43 9	00 00 01 4		Mylonite	028	78	E	CLEAVAGE		066
066	14 36 43 9	00 00 01 4		Mylonite		12	028	LINEATION		
067	14 35 47 3			Mylonitised granitoid	034	78	E	CLEAVAGE		
068	14 36 43 9		00 00 17 4	Mylonitised granitoid	026	75	E	CLEAVAGE		068
068	14 36 43 9		00 00 17 4	Mylonitised granitoid		64	113	LINEATION		068
069	14 36 35 6		00 00 16	Mylonitised granitoid	045	45	E	CLEAVAGE		

			6							
070	14 36 30 2		00 00 16 2	Mylonitised granitoid	071	72	E	CLEAVAGE		
070	14 36 30 2		00 00 16 2	Mylonitised granitoid		82	114	LINEATION		
070	14 36 30 2		00 00 16 2	Mylonitised granitoid	037	54	W	FAULT		
070	14 36 30 2		00 00 16 2	Mylonitised granitoid	283	53	W	FAULT		
070	14 36 30 2		00 00 16 2	Mylonitised granitoid	040	54	W	FAULT		
070	14 36 30 2		00 00 16 2	Mylonitised granitoid	080	51	W	FAULT		
071	14 36 50 4	00 00 18 6		Mylonitised ??	042	80	W	CLEAVAGE		071
071	14 36 50 4	00 00 18 6		Mylonitised ??		5	222	LINEATION		
072	14 37 30 0	00 00 25 4		Mylonitised ??	013	85	E	CLEAVAGE		
072	14 37 30 0	00 00 25 4		Mylonitised ??		85	012	LINEATION		
072	14 37 30 0	00 00 25 4		Mylonitised ??	010	82	W	CLEAVAGE		
072	14 37 30 0	00 00 25 4		Mylonitised ??		18	014	LINEATION		
073	14 37 25 9	00 00 09 1		Mylonitised Adamelite granite	037	72	E	CLEAVAGE		
073	14 37 25 9	00 00 09 1		Mylonitised Adamelite granite		71	126	LINEATION		
074	14 37 05 7		00 00 40 2	Adamelite granite						074
075	14 36 31 8		00 00 45 2	Adamelite granite	050	84	E	CLEAVAGE		
075	14 36 31 8		00 00 45 2	Adamelite granite		87	141	LINEATION		
076	14 36 15 9		00 01 25	Adamelite granite	008	90		CLEAVAGE		

			9							
076	14 36 15 9		00 01 25 9	Adamelite granite		44	116	LINEATION		
077	14 35 53 0		00 01 45 1	Adamelite granite	284	58	S	CLEAVAGE		
077	14 35 53 0		00 01 45 1	Adamelite granite		80	206	LINEATION		
078	14 46 49 8	00 02 14 6		Tambao granodiorite	246			TREND		
079	14 47 23 5	00 03 45 5		Tambao manganese deposit						
080	14 47 09 7	00 03 12 6		Buck-quartz carbonate vein	082			TREND		080
081	14 37 35 7	00 00 32 6		Chlorite mica schist	025			TREND		081
082	14 37 25 8	00 00 23 2		Mylonitised ??						
083	13 59 56 2		00 01 37 4	Tonalite	098			TREND		
084	13 59 40 4	00 19 31 2		Granodiorite	012			TREND		
085	14 34 10 4		00 00 48 7	Laterite						
086	14 34 14 7		00 00 49 3	Hornfels	284			TREND		086
086	14 34 14 7		00 00 49 3		275	84	S			
087	14 34 14 7		00 00 49 3	Gabbro contact aureole zone						
088	14 34 08 8		00 01 00 0	Laterite						
089	14 34 12 9		00 01 10 6	Norite	038	68	W	ELONGATION		
089	14 34 12 9		00 01 10 6	Norite	057	52	W	CLEAVAGE		
089	14 34 12 9		00 01 10	Norite	047	71	W	CLEAVAGE		

			6							
089	14 34 12 9		00 01 10 6	Norite	054	68	W	CLEAVAGE		
089	14 34 12 9		00 01 10 6	Norite	062	78	W	CLEAVAGE		
089	14 34 12 9		00 01 10 6	Norite	036	75	W	CLEAVAGE		
090	14 33 59 3		00 00 53 2	Laterite						
091	14 34 23 5		00 00 39 9	Mylonitised ??	017	77	E	CLEAVAGE		091
091	14 34 23 5		00 00 39 9	Mylonitised ??		21	197	LINEATION		091
092	14 34 31 7		00 00 44 5	Noritic granodiorite-tonalite	028	80	E	CLEAVAGE		092
092	14 34 31 7		00 00 44 5	Noritic granodiorite-tonalite	070	61	E	CLEAVAGE		
093	14 34 33 3		00 00 49 1	Noritic granodiorite-tonalite						
094	14 34 36 8		00 00 54 3	Proto L-tectonite zone	352			TREND		
094	14 34 36 8		00 00 54 3	Proto L-tectonite zone		69	262	LINEATION		
094	14 34 36 8		00 00 54 3	Proto L-tectonite zone		67	124	LINEATION		
094	14 34 36 8		00 00 54 3	Proto L-tectonite zone		55	147	LINEATION		
095	14 34 34 0		00 00 53 1	Proto L-tectonite zone						095
096				No data						
097	14 34 53 3		00 00 39 5	Granodiorite-tonalite	051	72	E	CLEAVAGE		
097	14 34 53 3		00 00 39 5	Granodiorite-tonalite		24	215	LINEATION		
098	14 35 11 5		00 00 36 0	Noritic granodiorite-tonalite						098

099	14 35 05 7		00 00 05 4	Granodiorite-tonalite						
100	14 34 59 9	00 00 07 9		Granodiorite-tonalite	014	81	W	CLEAVAGE		100
100	14 34 59 9	00 00 07 9		Granodiorite-tonalite	014	77	W	CLEAVAGE		
100	14 34 59 9	00 00 07 9		Granodiorite-tonalite	010	77	W	CLEAVAGE		
100	14 34 59 9	00 00 07 9		Granodiorite-tonalite	035	75	E	CLEAVAGE		
100	14 34 59 9	00 00 07 9		Granodiorite-tonalite	015	47	E	CLEAVAGE		
100	14 34 59 9	00 00 07 9		Granodiorite-tonalite	008	83	W	CLEAVAGE		
100	14 34 59 9	00 00 07 9		Granodiorite-tonalite	356	78	W	CLEAVAGE		
100	14 34 59 9	00 00 07 9		Granodiorite-tonalite	021	64	W	CLEAVAGE		
101	14 34 49 1	00 00 04 6		Chlorite-quartz mica schist	027	57	W	CLEAVAGE		
101	14 34 49 1	00 00 04 6				54	275	LINEATION		
102	14 35 02 3	00 00 13 1		Schistosed	020	48	E	CLEAVAGE		
102	14 35 02 3	00 00 13 1		Schistosed	010	58	W	CLEAVAGE		
103	14 35 02 3	00 00 13 1		Quartz-carbonate vein	303			TREND		
104	14 36 45 6	00 00 32 3		Tonalite	315	70	E	ELONGATION		
104	14 36 45 6	00 00 32 3		Tonalite	317	83	E	ELONGATION		
105	14 37 25 5	00 06 23 5		Mylonite	010	66	W	CLEAVAGE		
105	14 37 25 5	00 06 23 5		Mylonite		10	000	LINEATION		

106	14 37 25 8	00 00 02 1		Mylonitised Adamelite granite	027	88	E	CLEAVAGE		
106	14 37 25 8	00 00 02 1		Mylonitised Adamelite granite	356	81	S	FRACTURE		
107	14 34 23 4	00 00 20 4		Mylonitised Adamelite granite	041	71	W	CLEAVAGE		
107	14 34 23 4	00 00 20 4		Mylonitised Adamelite granite		8	041	LINEATION		
107	14 34 23 4	00 00 20 4		Mylonitised Adamelite granite	002	86	W	FRACTURE		
108	14 37 25 9	00 00 05 6		Mylonitised Adamelite granite	011	73	E	CLEAVAGE		
108	14 37 25 9	00 00 05 6		Mylonitised Adamelite granite		78	102	LINEATION		
109	14 37 23 1	00 00 05 6		Mylonitised Adamelite granite	050	77	E	CLEAVAGE		109
109	14 37 23 1	00 00 05 6		Mylonitised Adamelite granite		76	111	LINEATION		
110	14 22 44 2	00 04 42 4		Siltstone-sandstone greywacke-shale sequence	340	42	E	BEDDING		
111	14 23 01 9	00 04 27 5		Saprolite profile						
112	14 24 40 1	00 03 33 5		Essakane trench						
113				Buck-quartz carbonate vein	006			PDZ		
113	14 27 21 8		00 00 18 5	Buck-quartz carbonate vein	332			TREND		
113	14 27 19 4		00 00 19 0	Buck-quartz carbonate vein		60	214	LINEATION		
113	14 27 19 4		00 00 19 0	Buck-quartz carbonate vein		62	228	LINEATION		
113	14 27 19 4		00 00 19 0	Buck-quartz carbonate vein		63	226	LINEATION		
113	14 27 19 4		00 00 19 0	Buck-quartz carbonate vein		55	221	LINEATION		
113	14 27 14 5		00 00 19	Buck-quartz carbonate vein						

			6							
114	14 27 06 8		00 00 35 9	Buck-quartz carbonate vein	026	82	W	CLEAVAGE		
115	14 27 01 3		00 00 33 4	Sandstone greywacke	022	78	W	CLEAVAGE		
116				Poneere trend						
116A	14 26 22 3		00 00 16 3	Siltstone	028			TREND		
116A	14 26 24 0		00 00 15 5	Siltstone	066	82	S	CLEAVAGE		
116A	14 26 21 3		00 00 16 7	Siltstone	050	86	S	CLEAVAGE		
116A					073	72	S	CLEAVAGE		
116A						82	173	LINEATION		
116A					060	71	S	CLEAVAGE		
116B	14 26 26 1		00 00 16 0	Buck-quartz carbonate vein	038	77	E	CLEAVAGE		
116B	14 26 26 1		00 00 15 4	Buck-quartz carbonate vein						
116B	14 26 27 4		00 00 15 0	Buck-quartz carbonate vein	035	52	E	CLEAVAGE		116 C
116B	14 26 29 6		00 00 14 8	Buck-quartz carbonate vein						
116B	14 26 30 5		00 00 15 8	Buck-quartz carbonate vein						
116B	14 26 32 2		00 00 15 1	Buck-quartz carbonate vein	041			TREND		
116B					075	84	E	CLEAVAGE		
116B	14 26 32 2		00 00 16 3	Buck-quartz carbonate vein	017			TREND		
116B	14 26 40 0		00 00 14 2	Buck-quartz carbonate vein	035			TREND		
116B	14 26 47 4		00 00 13 3	Buck-quartz carbonate vein	034			TREND		
117	14 22 42 1	00 04 33 2		Exploration trench in Essakane 1	060			TREND		

117	14 22 43 9	00 04 42 5		End of north wall						
117	14 22 42 6	00 04 40 3		Start os south wall mosaic	090			TREND		
117	14 22 42 8	00 04 40 8		End of south wall (Siltstone) mosaic	350	42	E	BEDDING	E	
117					332	88	E	FAULT		
117				Sandstone greywacke	340	46	E	BEDDING		
118	14 22 42 8	00 04 39 3		Western limb of the anticline	327	24	W	BEDDING	W	
119	14 22 42 4	00 04 33 2			358	58	W	BEDDING	W	
120	14 22 42 6	00 04 39 7			340	71	W	BEDDING	W	
121	14 22 43 0	00 04 38 6			089	23	N	BEDDING		
122	14 22 43 3	00 04 40 4			024	42	E	BEDDING	E	
123	14 22 43 3	00 04 41 4			339	31	E	BEDDING	E	
124	14 22 44 1	00 04 42 2			340	42	E	BEDDING	E	
125	14 22 53 5	00 04 32 1		Exploration trench in Essakane 2	065			TREND		
125	14 22 54 5	00 04 34 1		End of north wall mosaic						
126	14 22 56 9	00 04 29 3		Exploration trench in Essakane 3	068			TREND		
126	14 22 58 8	00 04 33 7		End of north wall mosaic						
127	14 22 39 8		00 03 15 8	Sandstone greywacke (volcanoclastic)	070	48	S			
				ALLUVIAL PROFILE						